AD-A075 521 NATIONAL AVIATION FACILITIES EXPERIMENTAL CENTER ATL--ETC F/G 17/7
COMPUTER STUDY OF TULSA INTERNATIONAL AIRPORT RUNWAY 17R GLIDE --ETC(U)
SEP 79 T J LAGINJA

UNCLASSIFIED FAA-NA-79-8 FAA-RD-79-27 NL

1 OF 1
AD A075521

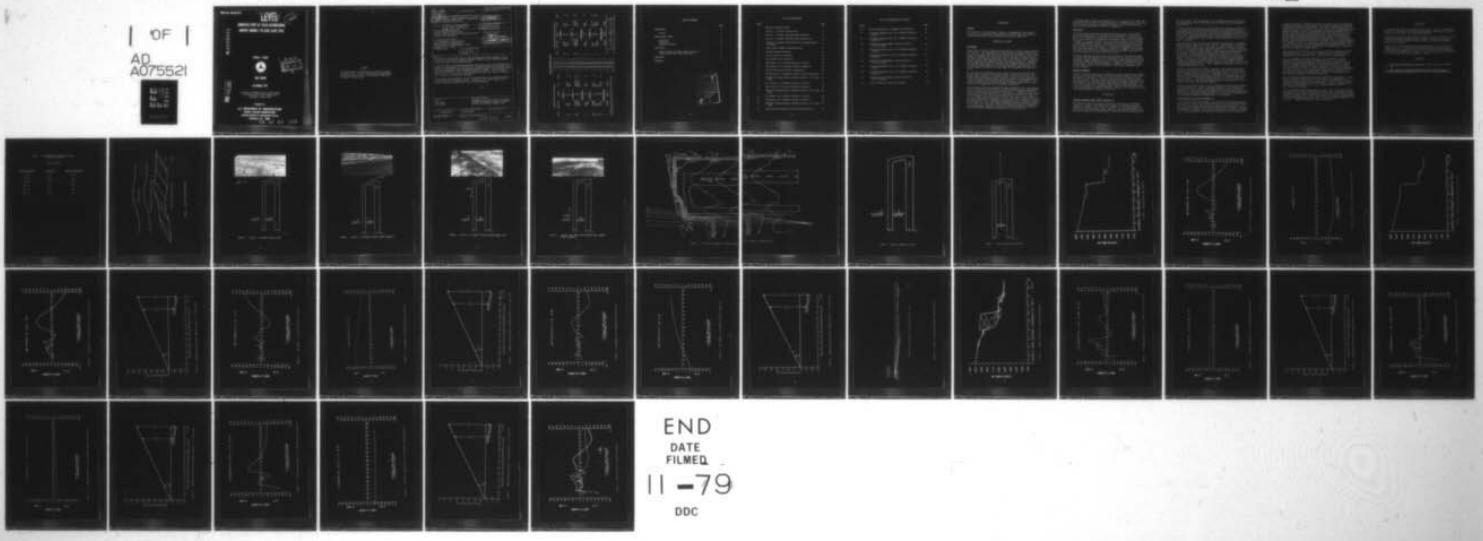

END
DATE FILMED
11-79
DDC

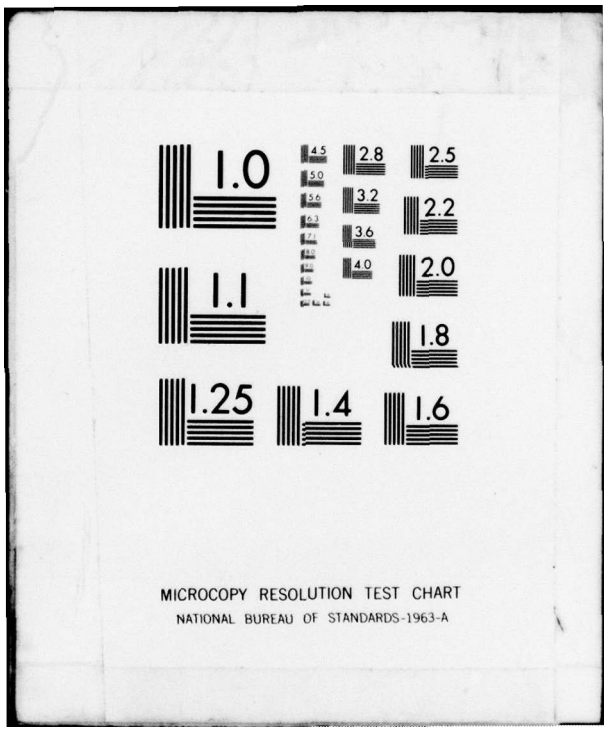
1.0
1.1
1.25
1.4
1.6
1.8
2.0
2.2
2.5
2.8
3.2
3.6
4.0
4.5
5.0
5.6
6.3
MICROCOPY RESOLUTION TEST CHART
NATIONAL BUREAU OF STANDARDS-1963-A

Report No. FAA-RD-79-27

LEVEL II

12

B.S.

# COMPUTER STUDY OF TULSA INTERNATIONAL AIRPORT RUNWAY 17R GLIDE SLOPE SITES



Thomas J. Laginja



FINAL REPORT

SEPTEMBER 1979





Prepared for

U.S. DEPARTMENT OF TRANSPORTATION
FEDERAL AVIATION ADMINISTRATION
Systems Research & Development Service
Washington, D.C. 20590

NOTICE

The United States Government does not endorse products or manufacturers. Trade or manufacturer's names appear herein solely because they are considered essential to the object of this report.

**Technical Report Documentation Page**

| 1. Report No. | 2. Government Accession No. | 3. Recipient's Catalog No. |
|---|---|---|
| FAA-RD-79-27 | | |

| 4. Title and Subtitle | 5. Report Date |
|---|---|
| COMPUTER STUDY OF TULSA INTERNATIONAL AIRPORT RUNWAY 17R GLIDE SLOPE SITES | September 1979 |
| | 6. Performing Organization Code |

| 7. Author(s) | 8. Performing Organization Report No. |
|---|---|
| Thomas J. Laginja | FAA-NA-79-8 |

| 9. Performing Organization Name and Address | 10. Work Unit No. (TRAIS) |
|---|---|
| Federal Aviation Administration<br>National Aviation Facilities Experimental Center<br>Atlantic City, New Jersey | 11. Contract or Grant No.<br>071-713-800 |

| 12. Sponsoring Agency Name and Address | 13. Type of Report and Period Covered |
|---|---|
| U.S. Department of Transportation<br>Federal Aviation Administration<br>Systems Research and Development Service<br>Washington, D.C. 20590 | Final rept.<br>Feb[illegible]-Nov[illegible] 1978 |
| | 14. Sponsoring Agency Code |

15. Supplementary Notes

12 46

16. Abstract

The terrain at the approach end of Tulsa International Airport Runway 17R is of concern as to its effect on guidance signals radiated from an instrument landing system (ILS) glide slope antenna system.

In order to select the antenna system that will result in the least perturbation of signal, the performances of Capture Effect, Sideband Reference, and Null Reference systems were compared using a mathematical simulation model on the National Aviation Facilities Experimental Center's (NAFEC) Honeywell computer. Since the mathematical model has not, as yet, been validated, the simulation results presented in this report are considered as preliminary.

Results show that performance, for both the Capture Effect and Sideband Reference systems were within Category I limits. Overall, a 2.8° capture effect system located outside the taxiway offers the best performance.

dey

| 17. Key Words | 18. Distribution Statement |
|---|---|
| ILS<br>Math Model<br>Glide Slope | Document is available to the U.S. public through the National Technical Information Service, Springfield, Virginia 22151 |

| 19. Security Classif. (of this report) | 20. Security Classif. (of this page) | 21. No. of Pages | 22. Price |
|---|---|---|---|
| Unclassified | Unclassified | 42 | |

Form DOT F 1700.7 (8-72) Reproduction of completed page authorized

240 550

# METRIC CONVERSION FACTORS

## Approximate Conversions to Metric Measures

| Symbol | When You Know | Multiply by | To Find | Symbol |
|---|---|---|---|---|
| | | **LENGTH** | | |
| in | inches | *2.5 | centimeters | cm |
| ft | feet | 30 | centimeters | cm |
| yd | yards | 0.9 | meters | m |
| mi | miles | 1.6 | kilometers | km |
| | | **AREA** | | |
| $in^2$ | square inches | 6.5 | square centimeters | $cm^2$ |
| $ft^2$ | square feet | 0.09 | square meters | $m^2$ |
| $yd^2$ | square yards | 0.8 | square meters | $m^2$ |
| $mi^2$ | square miles | 2.6 | square kilometers | $km^2$ |
| | acres | 0.4 | hectares | ha |
| | | **MASS (weight)** | | |
| oz | ounces | 28 | grams | g |
| lb | pounds | 0.45 | kilograms | kg |
| | short tons (2000 lb) | 0.9 | tonnes | t |
| | | **VOLUME** | | |
| tsp | teaspoons | 5 | milliliters | ml |
| Tbsp | tablespoons | 15 | milliliters | ml |
| fl oz | fluid ounces | 30 | milliliters | ml |
| c | cups | 0.24 | liters | l |
| pt | pints | 0.47 | liters | l |
| qt | quarts | 0.95 | liters | l |
| gal | gallons | 3.8 | liters | l |
| $ft^3$ | cubic feet | 0.03 | cubic meters | $m^3$ |
| $yd^3$ | cubic yards | 0.76 | cubic meters | $m^3$ |
| | | **TEMPERATURE (exact)** | | |
| °F | Fahrenheit temperature | 5/9 (after subtracting 32) | Celsius temperature | °C |

*1 in = 2.54 (exactly). For other exact conversions and more detailed tables, see NBS Misc. Publ. 286, Units of Weights and Measures, Price $2.25, SD Catalog No. C13.10:286.


## Approximate Conversions from Metric Measures

| Symbol | When You Know | Multiply by | To Find | Symbol |
|---|---|---|---|---|
| | | **LENGTH** | | |
| mm | millimeters | 0.04 | inches | in |
| cm | centimeters | 0.4 | inches | in |
| m | meters | 3.3 | feet | ft |
| m | meters | 1.1 | yards | yd |
| km | kilometers | 0.6 | miles | mi |
| | | **AREA** | | |
| $cm^2$ | square centimeters | 0.16 | square inches | $in^2$ |
| $m^2$ | square meters | 1.2 | square yards | $yd^2$ |
| $km^2$ | square kilometers | 0.4 | square miles | $mi^2$ |
| ha | hectares (10,000 $m^2$) | 2.5 | acres | |
| | | **MASS (weight)** | | |
| g | grams | 0.035 | ounces | oz |
| kg | kilograms | 2.2 | pounds | lb |
| t | tonnes (1000 kg) | 1.1 | short tons | |
| | | **VOLUME** | | |
| ml | milliliters | 0.03 | fluid ounces | fl oz |
| l | liters | 2.1 | pints | pt |
| l | liters | 1.06 | quarts | qt |
| l | liters | 0.26 | gallons | gal |
| $m^3$ | cubic meters | 35 | cubic feet | $ft^3$ |
| $m^3$ | cubic meters | 1.3 | cubic yards | $yd^3$ |
| | | **TEMPERATURE (exact)** | | |
| °C | Celsius temperature | 9/5 (then add 32) | Fahrenheit temperature | °F |

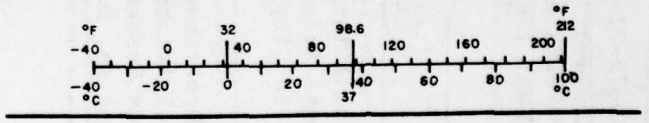

TABLE OF CONTENTS



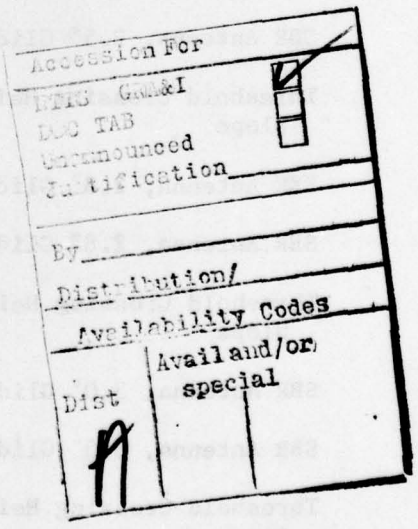

## LIST OF ILLUSTRATIONS

LIST OF ILLUSTRATIONS (Continued)

# INTRODUCTION

## PURPOSE.

The objective of this study was to provide a recommendation with respect to selection of an Instrument Landing System (ILS) Glide Slope system for the proposed installation on Tulsa International Airport runway 17R.

# DESCRIPTION OF MODEL

## BACKGROUND.

Runway 17R is 5,498 feet long by 150 feet wide and is used by general aviation type aircraft. The sharp dropoffs in terrain near the runway threshold area are cause for concern regarding glide slope system performance on this runway. Beyond the threshold area, the terrain is flat and void of irregularities. Mathematical modeling was employed in order to economically assess the performance of various glide slope systems at each of two sites on 17R. The mathematical computer model used was a glide slope model developed by Transportation Systems Center (TSC) and converted by the National Aviation Facilities Experimental Center (NAFEC) to its in-house Honeywell 66/60 computer. The set of programs included in this math model will, henceforth, be referred to as GSI.

The GSI model was developed by TSC as a means for analysis of airport topography effects on glide slope antenna systems. Since this model has only recently been converted to the NAFEC computer, there has not, as yet, been a validation program completed where simulation outputs have been compared with flight check data for given glide slope installations. While NAFEC is currently conducting such a validation program, results obtained prior to completion of the program must be considered as preliminary.

The GS1 model is but one of several ILS models developed by TSC. Descriptions of the ILS models and instructions for running the glide slope programs may be found in reports written by TSC (references 1 and 2). Inasmuch as the TSC reports carry detailed descriptions of the model, this report will limit itself to descriptions of the input data and output plots. While GS1 is limited in that it considers only terrain effects on the ILS signal, a newer version of the model, which shall be referred to as GS2, will, when in operation, consider scattering effects due to buildings, parked aircraft, etc., as well as terrain. At this time, GS2 is not operational and NAFEC and TSC are working to bring it "up" to where it can be used to model sites where buildings are a significant scattering concern. However, as terrain is the sole concern in the case of Tulsa 17R, GS1 was considered satisfactory for this application.

A localizer model has also been developed by TSC. This model has had some validation work done at NAFEC and is operational on the NAFEC computer. But, since Tulsa 17R does not present a problem with respect to localizer performance, only the glide slope model is used in the simulation.

INPUT DATA.

GS1 requires data inputs that describe the terrain in front of the antenna as well as descriptions of the antenna and the flightpath. The ground in front of the antenna must be described by parallel strips of infinite length. These strips, which run perpendicular to the runway centerline, are sketched in figure 1. In order to acquire input data for the model, a visit was made to Tulsa International Airport. The Airway Facilities Sector Office and the Southwest Region Office assisted by providing aerial photographs and contour maps of the area under consideration. In addition, photographs of the area were taken from the ground. Figures 2 through 6 are examples of the information acquired at Tulsa. The availability of such information precluded the need for a survey of the glide slope antenna area.

The antenna description consisted of the coordinates of each antenna element as well as real and imaginary current amplitudes for the carrier, 150 and 90 hertz (Hz) sideband frequencies. For this study, input parameters were chosen to provide various glidepath angles and a 1.4-degree (°) course width (full deflection 0.7° above or below glidepath). Flightpath description consisted of glide angle, starting point coordinates, ending point coordinates, and aircraft velocity.

MODELING TECHNIQUE.

For each receiver point along the flightpath, the model calculated the complex fields due to each antenna element for both the direct signal as well as for reflections off the ground. The sum of these direct and reflected signals was then input into receiver routines which calculated the receiver output in microamperes (μA). The model, which used dynamic smoothing, simulated an aircraft flying a hyperbolic glidepath aligned with the runway centerline. The output was evidence of the predicted course deviation indication (CDI) from 0 μA with the aircraft flying the hyperbolic approach. The computer processing time was approximately 5 minutes for each run.

## APPLICATION

SIDEBAND REFERENCE (SBR) SYSTEM (LOCATION 1).

Two possible locations for siting a glide slope antenna were investigated (figure 7). Location 1 was studied with respect to a sideband reference antenna installation. This location is 250 feet (ft) off runway centerline and 1,200 ft from the present runway threshold. Anticipated extension of the stop end of Runway 17R and displacement of threshold by 200 ft would position

the site 1,000 ft from the threshold. Due to height restrictions, neither the Capture Effect (CE) nor Null Reference (NR) antennas were considered for this location.

In order to model the terrain in front of this site, the land contour along a line parallel to the runway centerline (figure 8) was determined from the aerial photo/contour map. Figure 9 shows the terrain profile along this line. This profile was then broken down into straight line segments and entered into a data file. Simulation runs were made for glide slope angles of 2.5°, 2.8°, and 3.0°. Antenna heights were selected to provide glidepaths at the desired glide slope angles.

Figures 10 and 11 show the error plot obtained by running the 2.5° glidepath with SBR antenna heights of 5.95 and 17.85 ft. The plot shows a relatively constant error of about -25 μA from 40,000 to 25,000 ft where a slow bend begins. As the bend continues, the plot crosses 0 μA at 15,500 ft and swings to +22 μA at 11,500 ft. From 10,000 to 1,000 ft the error varies between -5 and +10 μA. This plot indicates marginal performance outside 10,000 ft. As an experiment, a depression in the ground near threshold was filled in (figure 12). The only noticeable difference in output was in the region of 5,000 to 1,000 ft. In that region, the error plot was flattened somewhat (figure 13). Threshold crossing heights for a 2.5° glide angle from this location are shown in figure 14. With threshold at its current location, the crossing height would be 66 ft. With a threshold displacement of 200 ft, the crossing height would be 54 ft.

Figures 15 and 16 show the results of running a 2.8° glidepath with antenna heights of 5.49 and 16.47 ft. These plots show a smooth rise from +13 to +25 μA between 40,000 and 22,000 ft. Following a drop to 0 μA at 14,500 ft, the error remains within ±13 μA for the remainder of the simulation. It is evident that a significant improvement over the 2.5° simulation takes place inside 15,000 ft. Threshold crossing heights for the 2.8° glidepath are shown in figure 17. The crossing height at present threshold is 73 ft and would be 60 ft with the threshold displaced.

Figures 18 and 19 show results of a 3.0° glidepath used with antenna heights of 5.22 and 15.66 ft. A smooth crossover from +18 to -17 μA takes place between 40,000 and 17,000 ft. Once inside 14,000 ft, the error does not exceed ±8 μA. This was the most satisfactory of the SBR antenna simulations. Figure 20 shows threshold crossing heights of 77 and 63 ft, respectively, for the present and displaced thresholds with a 3.0° glidepath.

CAPTURE EFFECT (CE) SYSTEM (LOCATION 2).

Location 2 was studied with respect to the CE, NR, and SBR antenna systems. This location is 600 ft from runway centerline (150 ft outside taxiway centerline) and 1,200 ft back from the present runway threshold (figure 1). The fact that GS1 recognizes only parallel terrain strips introduced a limitation in modeling this location. The runway and taxiway are situated on a plateau with a very sharp dropoff just beyond the threshold and a more gradual drop

alongside the taxiway. Therefore, a profile of terrain along a line parallel to runway centerline would be applicable only when the receiver is positioned a great distance from the antenna site. But, as the receiver moves toward the transmitting antenna, the terrain between the receiver and transmitting antenna appears to change. In order to approximate this situation with the model, a series of rays were drawn outward from the glide slope site (Location 2) at various angles to runway centerline (figure 21). The intersection of each ray with the extended runway centerline defined a point on the flightpath where the terrain profile along the same ray would apply. In all, six rays and six respective profiles were used in the model. The six profiles generated are overlayed in figure 22. Simulations were then run along selected profiles for the three systems at various antenna heights and glidepath angles. Preliminary runs showed the NR and SBR systems to be unsatisfactory. Therefore, only the CE system was studied further.

Simulations were run for each of the six profiles for CE systems with glide slope paths of 2.5°, 2.8°, and 3.0°. Composite plots were constructed by applying the output from each profile to its respective range segment.

The 2.5° glidepath, with antenna heights of 12.45, 24.90, and 37.40 ft, resulted in six profile outputs (one simulation run for each profile). Figures 23 and 24 show the composite plots constructed from the six profile plots. The composite plots indicate a relatively constant error of about +5 μA from 40,000 to 18,000 ft. After dropping to 0 μA error at 13,500 ft, the error rises to +12 μA at 12,500 ft, dips below 0 μA at 8,000 ft then rises to +26 μA at 6,200 ft. The sudden changes that take place inside 14,000 ft show less than satisfactory performance. Threshold crossing heights for a 2.5° system at Location 2 are shown in figure 25.

The 2.8° glidepath configuration provided a significant improvement. Antenna heights of 11.46, 22.92, and 34.38 ft were used. The composite plots (figures 26 and 27) show an error of less than 10 μA from 40,000 to 14,000 ft and an error not exceeding $\pm$ 15 μA from 14,000 to 2,000 ft. Figure 28 shows threshold crossing heights to be 65 ft at present threshold and 52 ft for a displaced threshold.

The 3.0° glidepath with antenna heights of 10.87, 21.75, and 32.62 ft yielded the composite plots shown in (figures 29 and 30). This output shows an error within 12 μA from 40,000 to 9,000 ft and then risings to +17 and -14 μA before stabilizing to within $\pm$5 μA from 4,500 to 2,000 ft. Threshold crossing heights for the 3.0° glidepath are found to be 70 ft for the present threshold and 55 ft for a displaced threshold as shown in figure 31.

## CONCLUSION

It should be noted that the mathematical model used to predict the performance data in this report has not, as yet, been validated. Therefore, the results presented in this report are considered preliminary.

Predictions for both the SBR system at Location 1 and the CE system at Location 2 indicate performance within Category I limits. Although the CE system provides the better performance outside 12,000 ft, the SBR system appears better inside 12,000 ft.

Overall, the 2.8° CE system located outside the taxiway offers the best performance while the 3.0° SBR system positioned between the runway and the taxiway is a close second choice. The outputs for both of these simulations are overlayed for comparison in figure 32. Standard deviations were calculated for each configuration and are presented in table 1.

## REFERENCES

1. ILS Glide Slope Performance Prediction, DOT/FAA, Report No. FAA-RD-74-157, 1974.

2. User's Manual For Generalized ILS GLD-ILS Glide Slope Performance Prediction: Multipath Scattering, DOT/FAA, Report No. FAA-RD-76-186, 1976.

TABLE 1. MEAN ERRORS AND STANDARD DEVIATIONS
(20,000 to 1,400 ft)

84 DATA POINTS

| System (degrees) | Mean (μA) | Standard Deviations |
|---|---|---|
| CE 2.5 | 4.72 | 6.59 |
| CE 2.8 | -4.40 | 7.35 |
| CE 3.0 | -2.78 | 8.71 |
| SBR 2.5 | 1.75 | 11.44 |
| SBR 2.8 | 2.62 | 9.76 |
| SBR 3.0 | -3.80 | 8.04 |

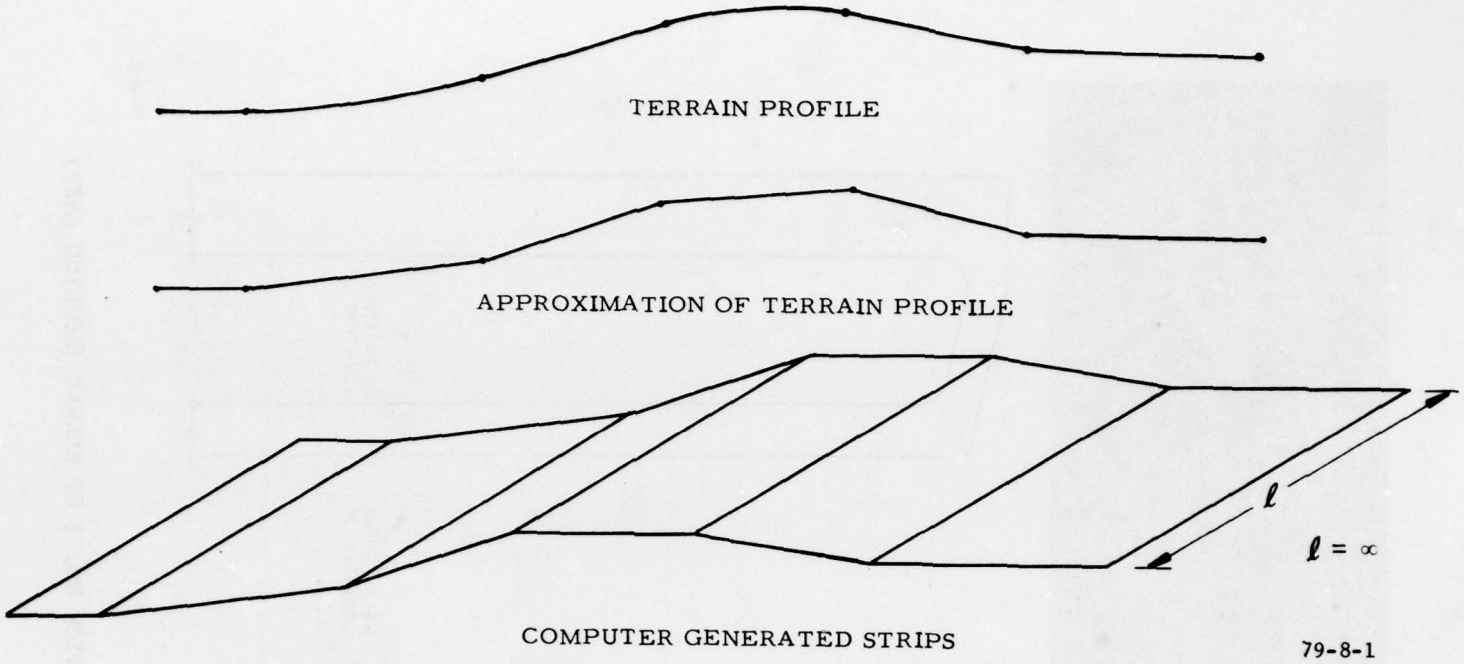


FIGURE 1. METHOD OF MODELING TERRAIN

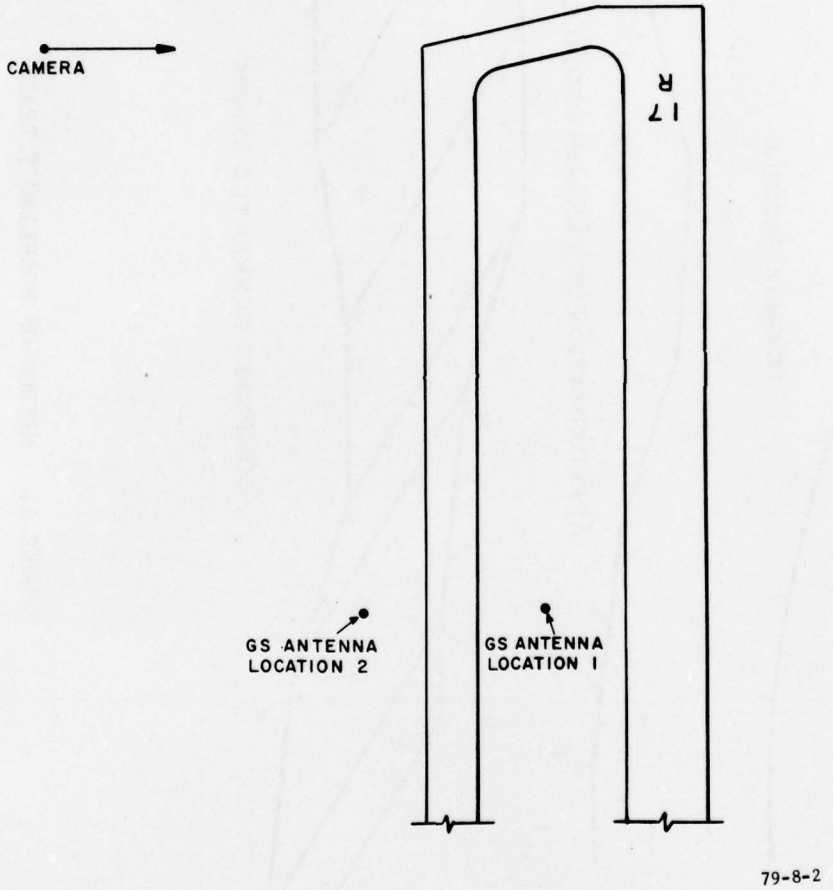


FIGURE 2. VIEW NO. 1 OF RUNWAY (LOOKING EAST)

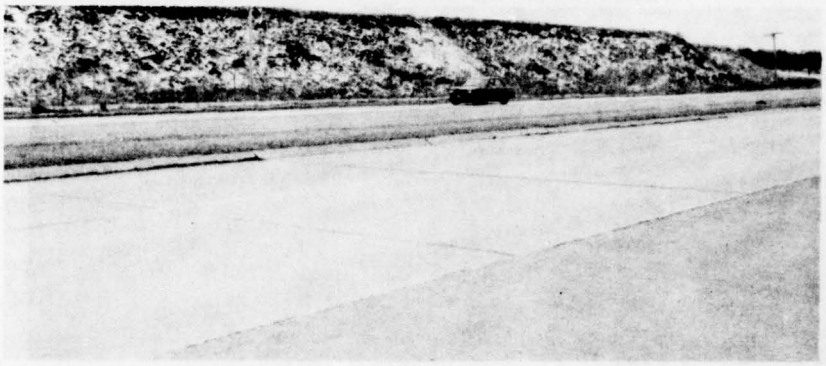

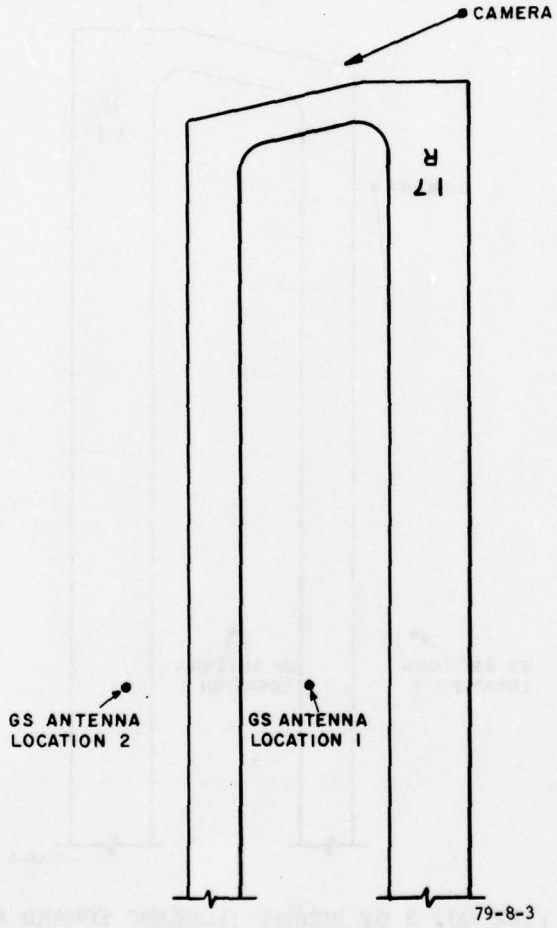


FIGURE 3. VIEW NO. 2 OF RUNWAY (LOOKING TOWARD THRESHOLD)

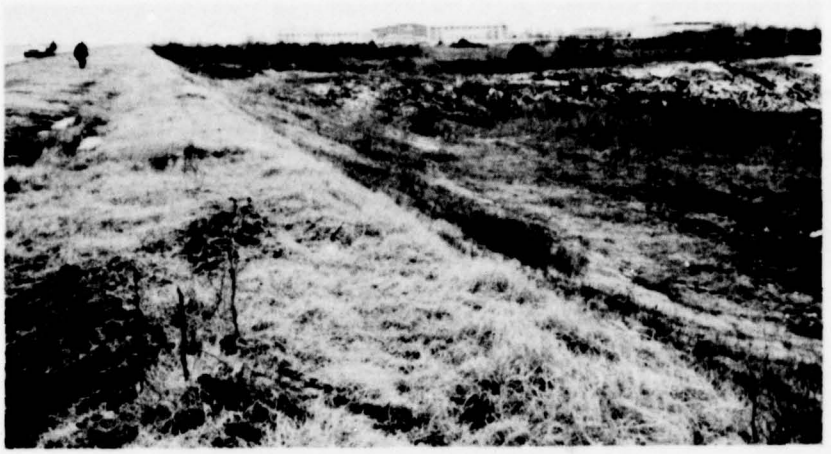

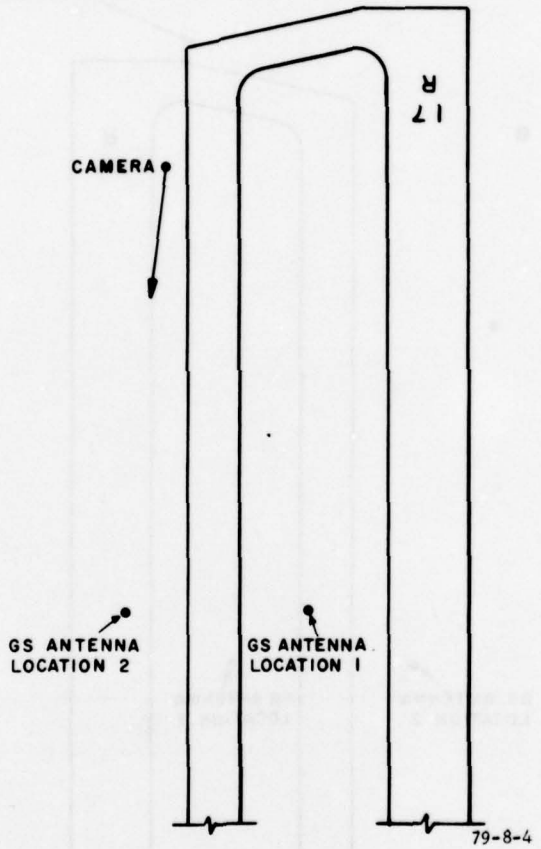


FIGURE 4. VIEW NO. 3 OF RUNWAY (LOOKING TOWARD ANTENNA SITE)

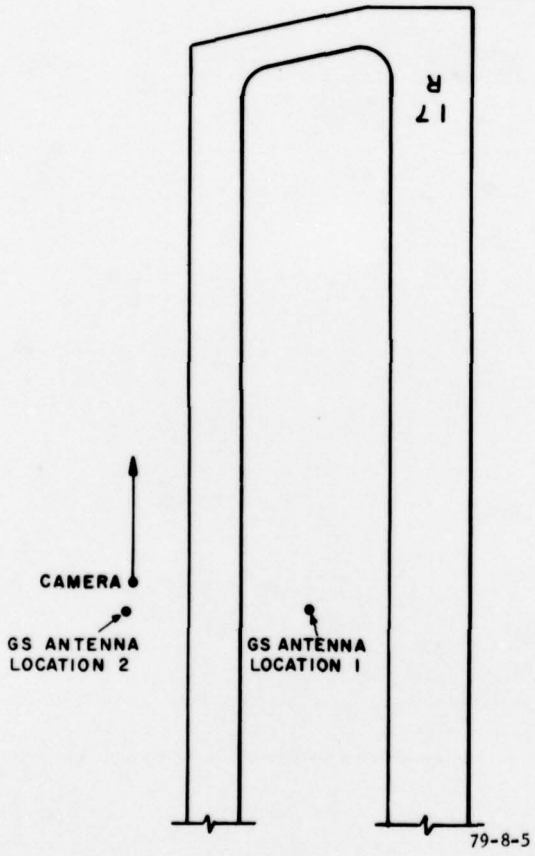


FIGURE 5. VIEW NO. 4 OF RUNWAY (FROM ANTENNA SITE, LOOKING TOWARD THRESHOLD)

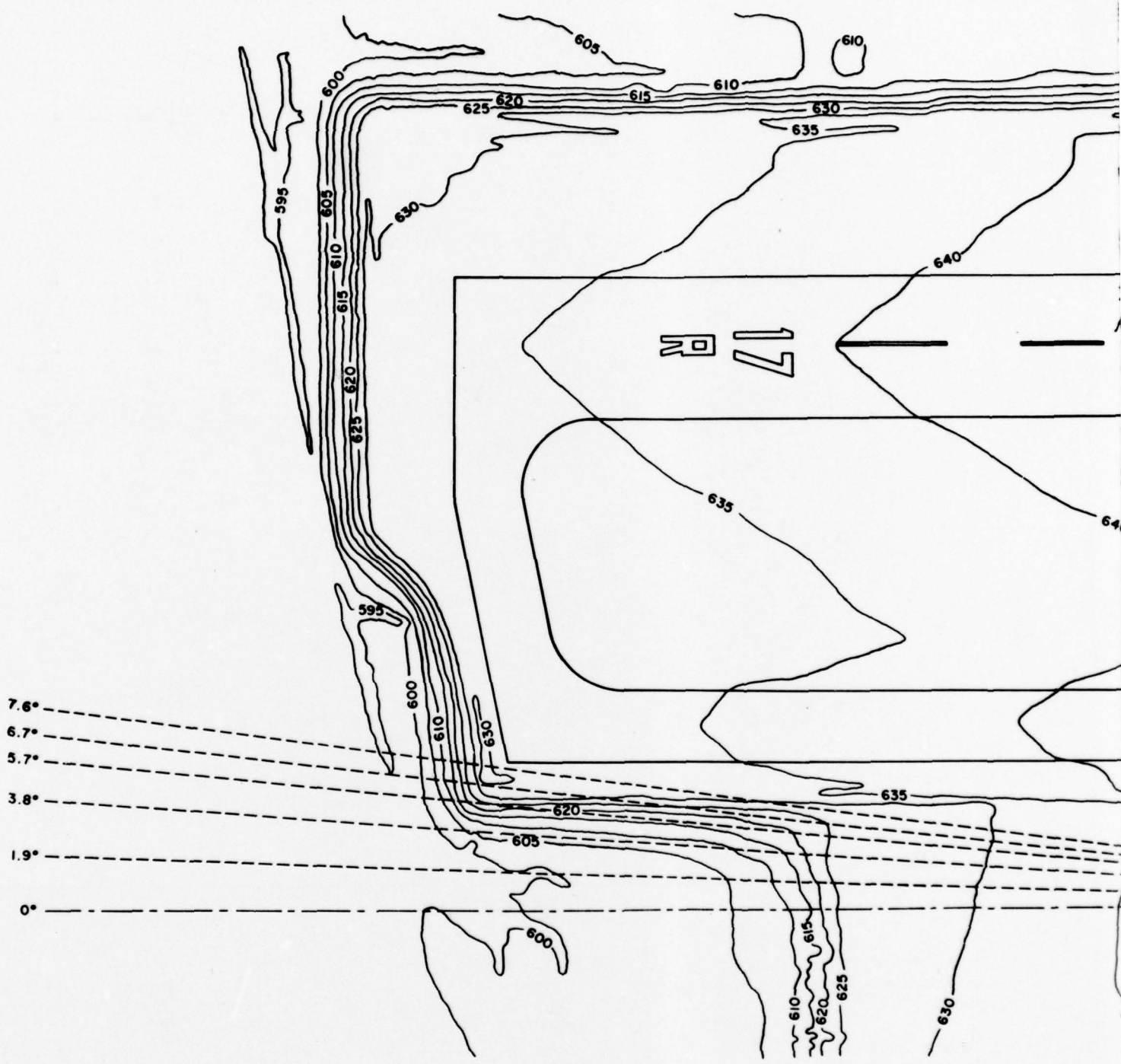


FIGURE 6. CONTOUR MAP OF RUNWAY 17R THRESHOLD AREA

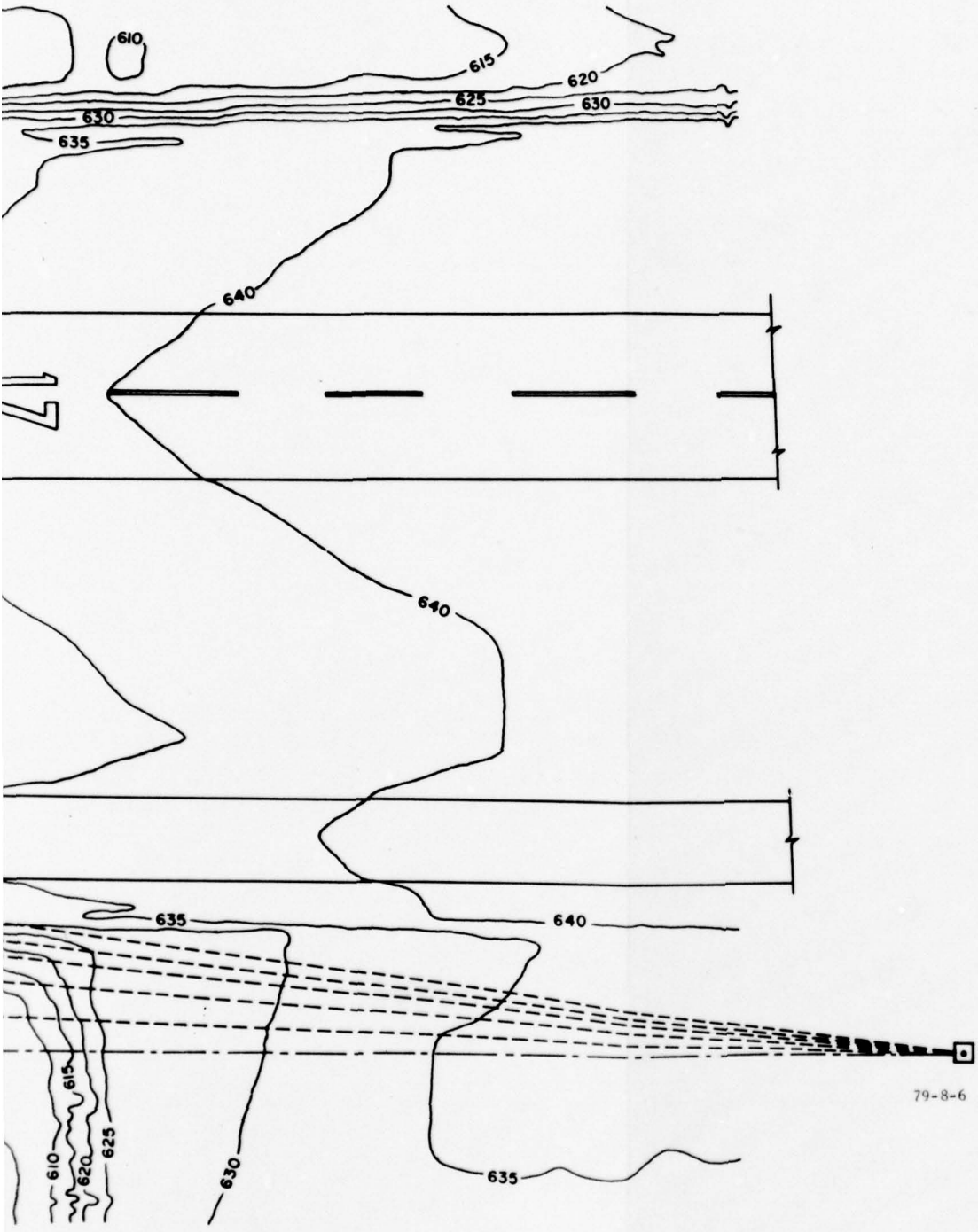


MAP OF RUNWAY 17R THRESHOLD AREA

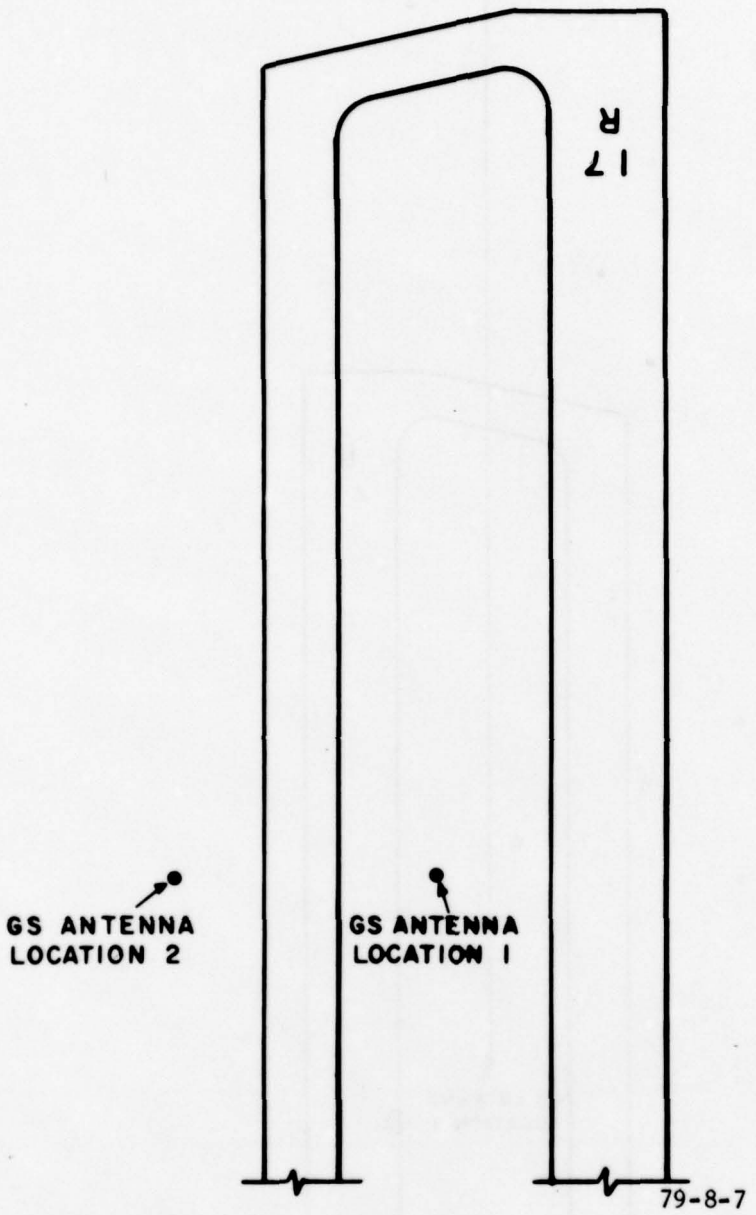


FIGURE 7. CANDIDATE ANTENNA LOCATIONS

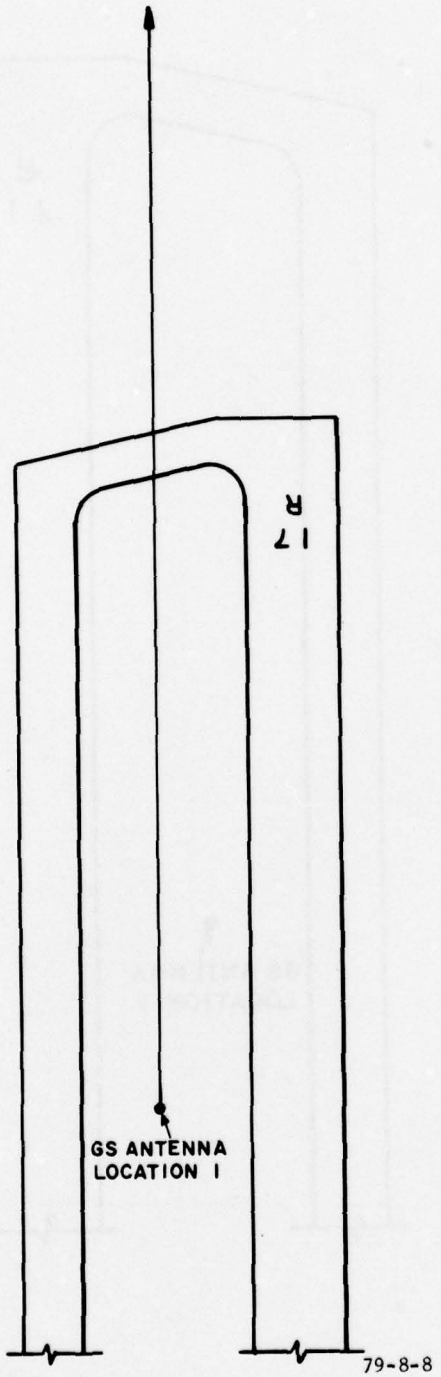


FIGURE 8. LINE OF PROFILE FOR LOCATION 1

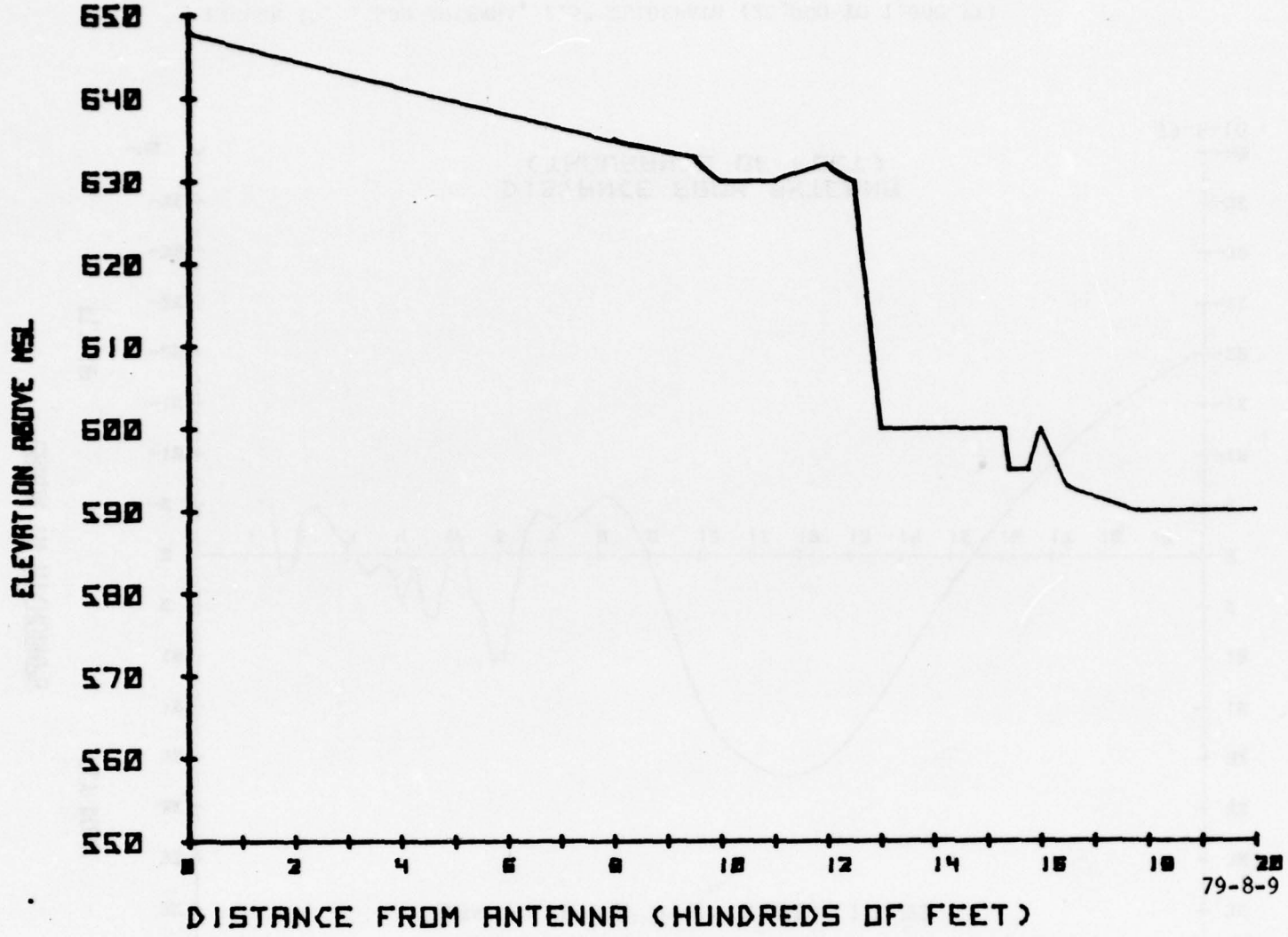


FIGURE 9. TERRAIN PROFILE FOR LOCATION 1

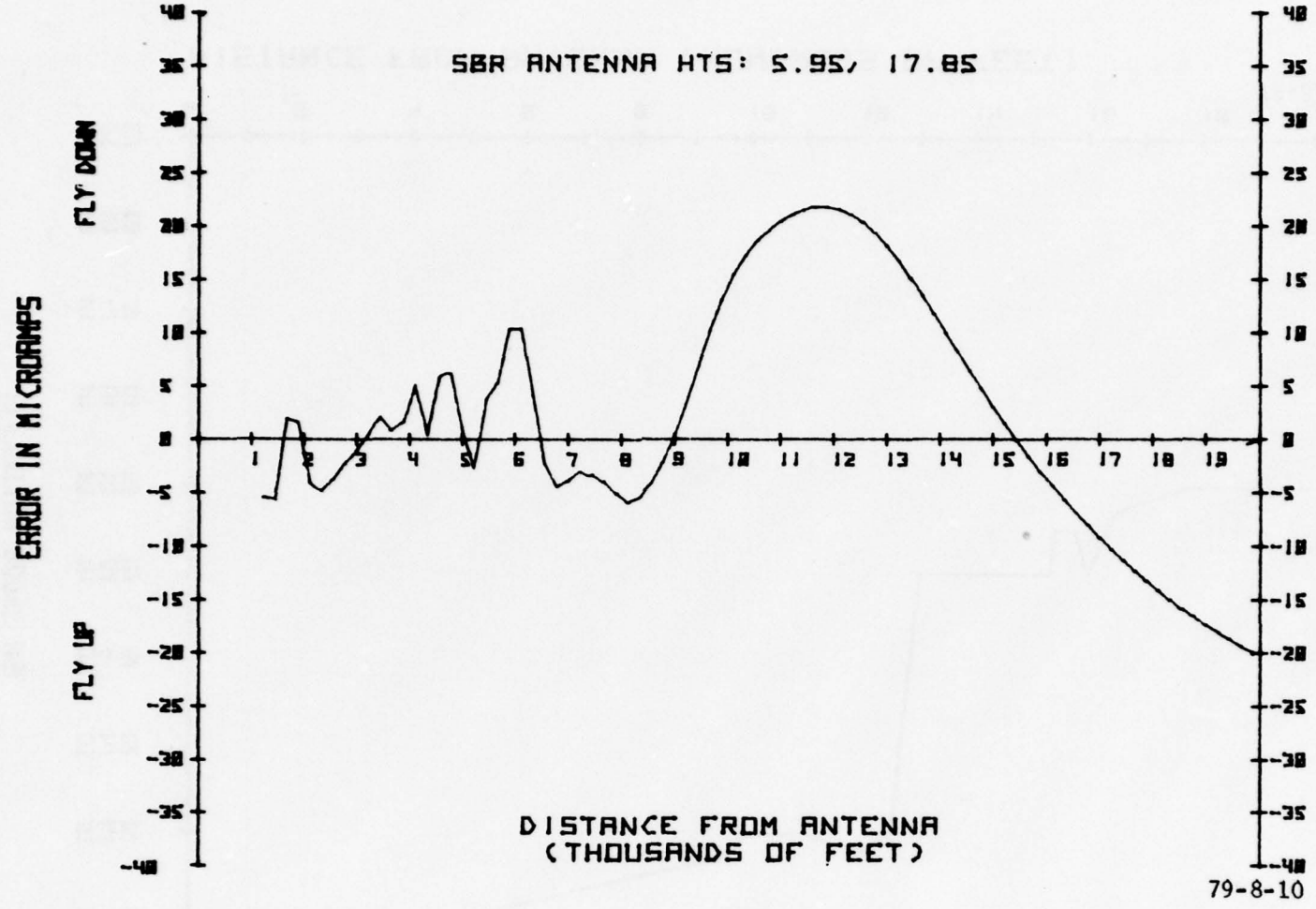


FIGURE 10. SBR ANTENNA, 2.5° GLIDEPATH (20,000 TO 1,000 FT)

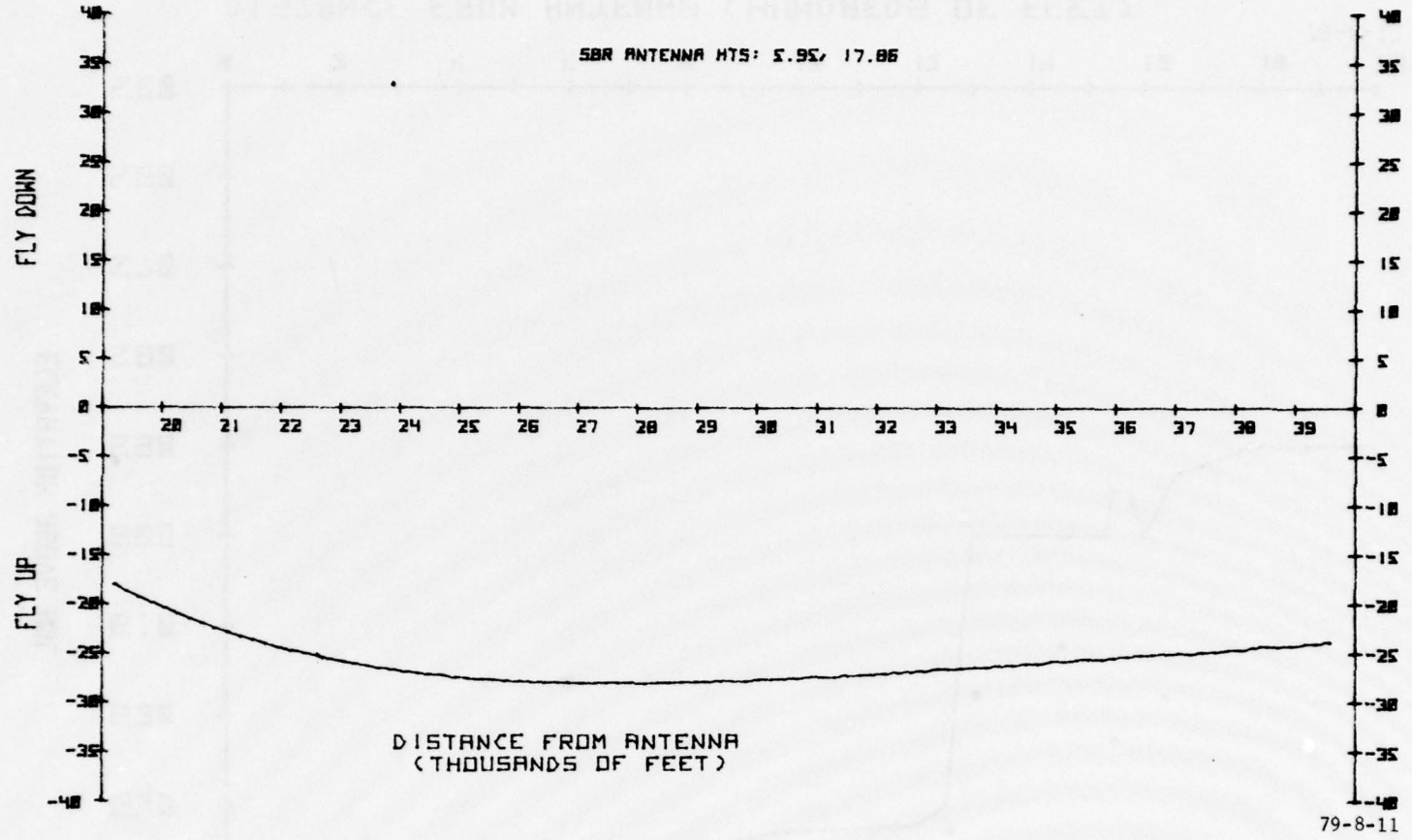


FIGURE 11. SBR ANTENNA, 2.5° GLIDEPATH (40,000 TO 20,000 FT)

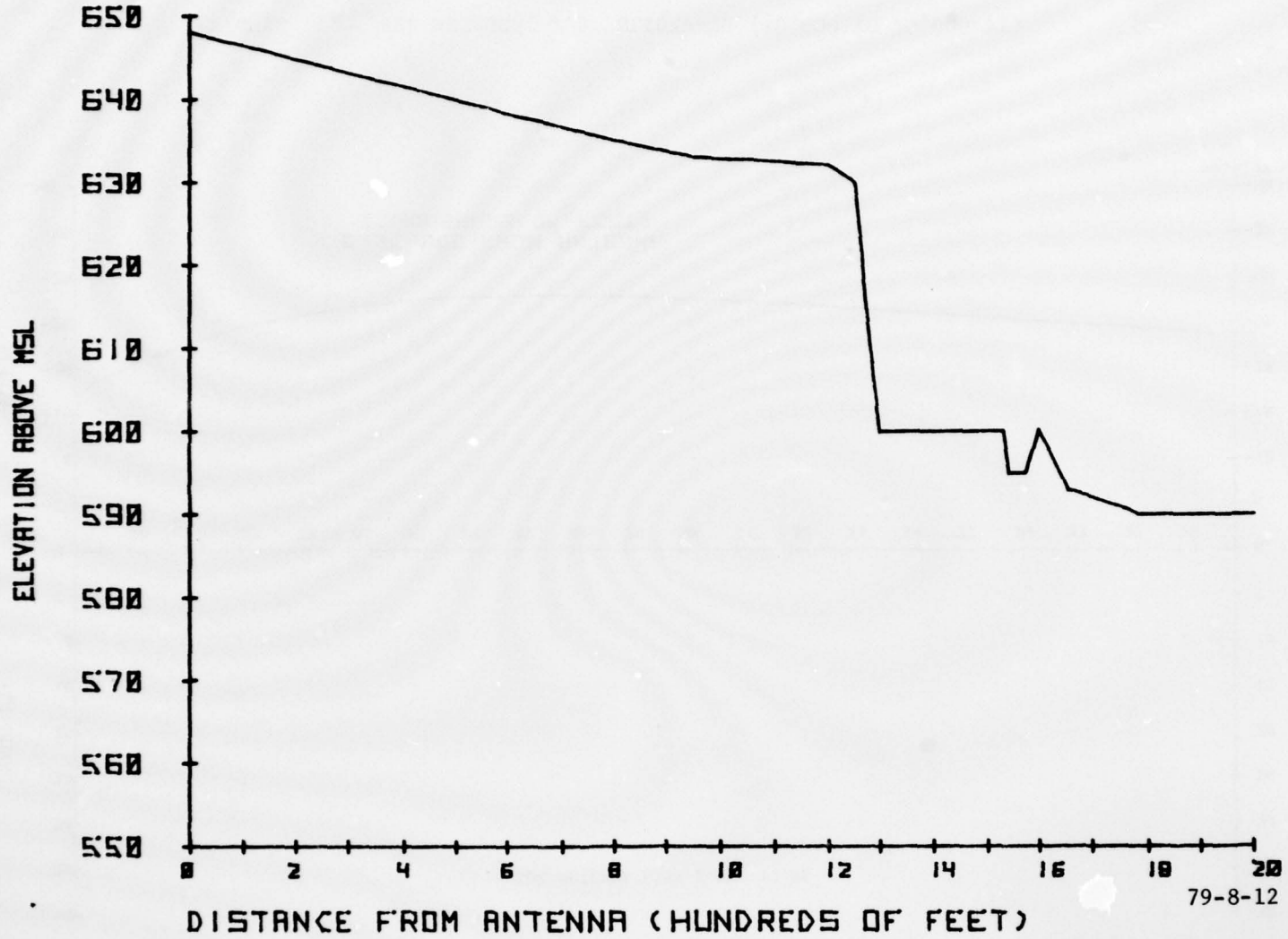


FIGURE 12. TERRAIN PROFILE FOR LOCATION 1 (WITH FILL)

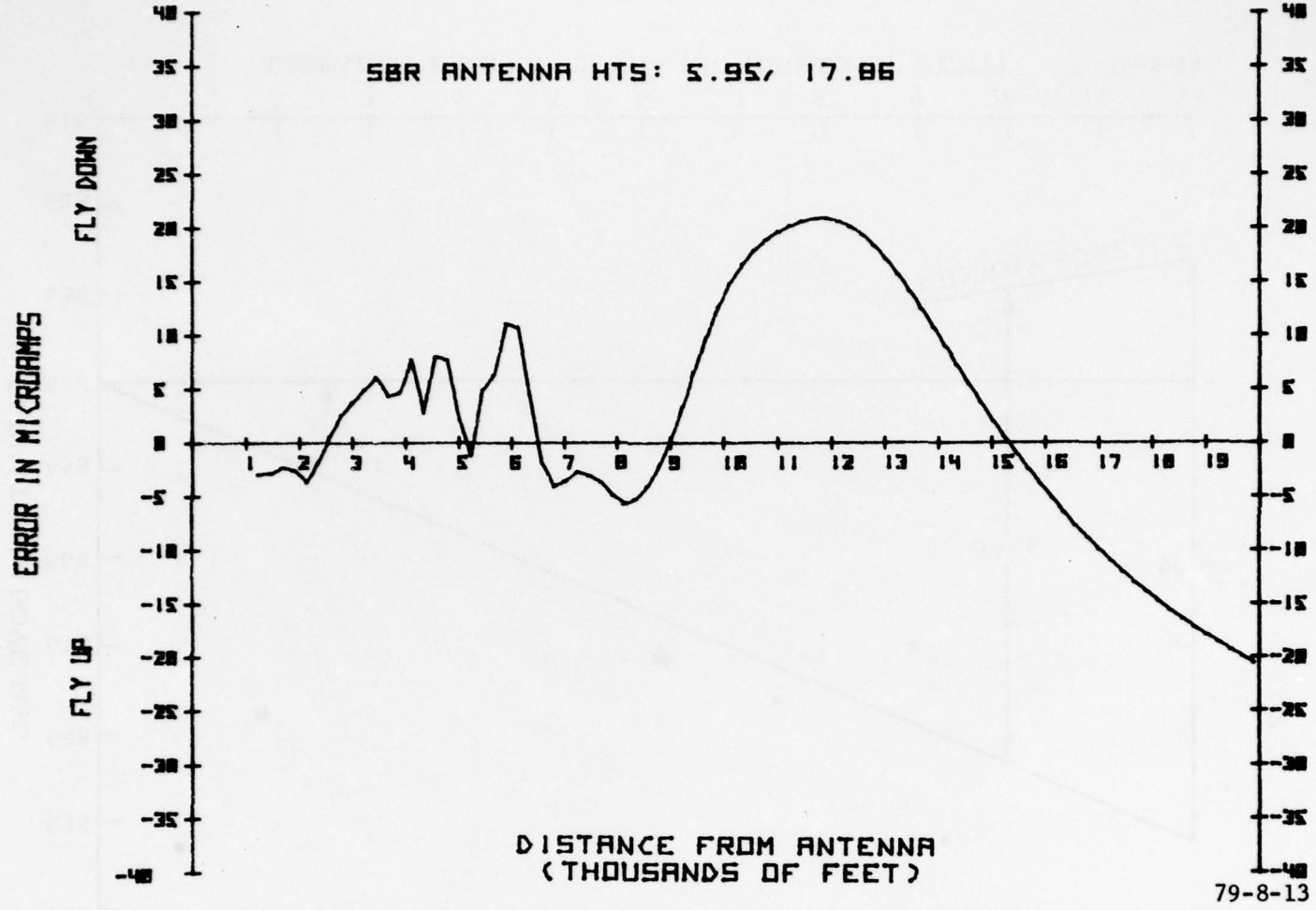


FIGURE 13. SBR ANTENNA, 2.5° GLIDEPATH (20,000 TO 1,000 FT WITH FILL)

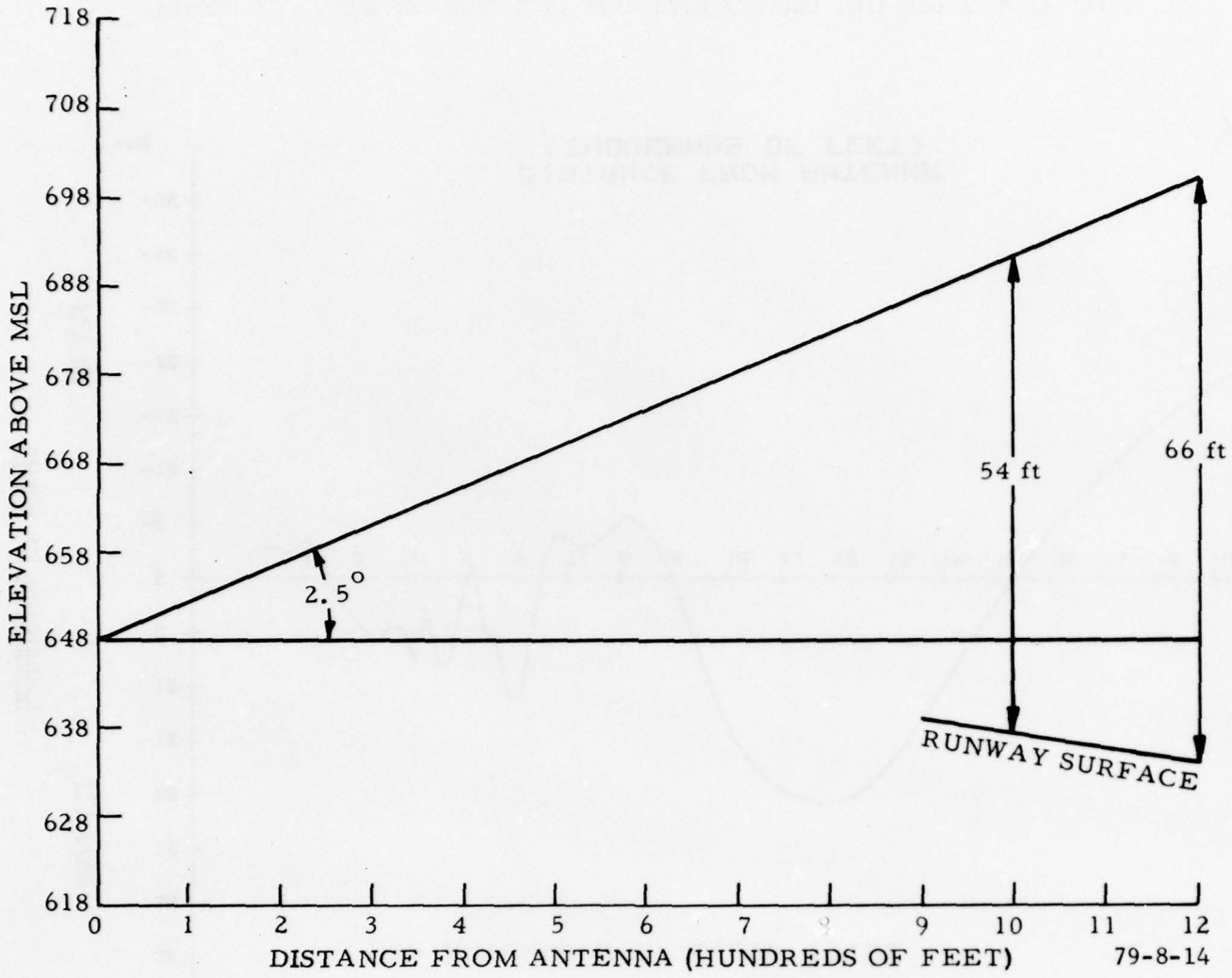


FIGURE 14. THRESHOLD CROSSING HEIGHTS, ANTENNA LOCATION 1, 2.5° GLIDE SLOPE

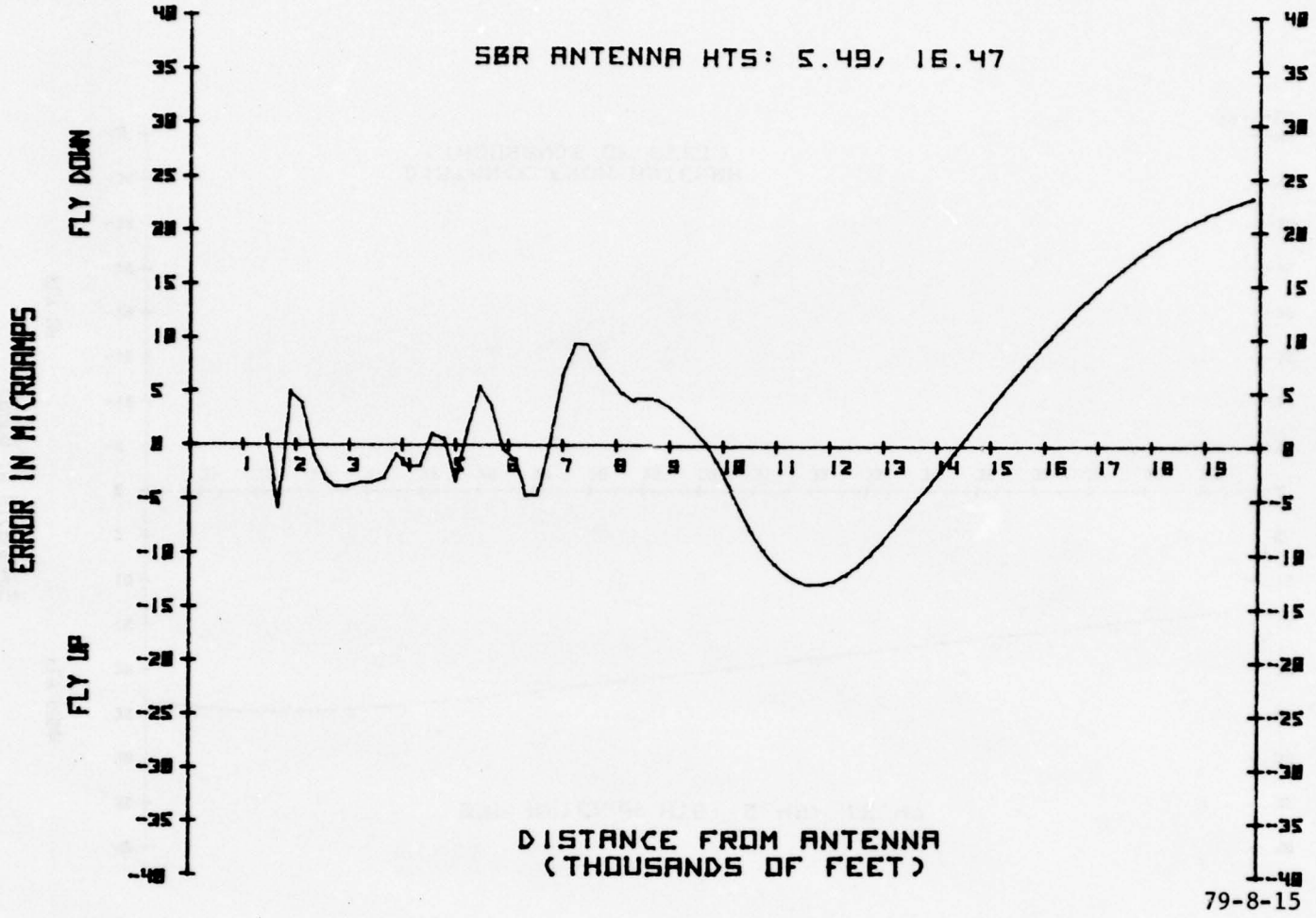


FIGURE 15. SBR ANTENNA, 2.8° GLIDEPATH (20,000 to 1,000 FT)

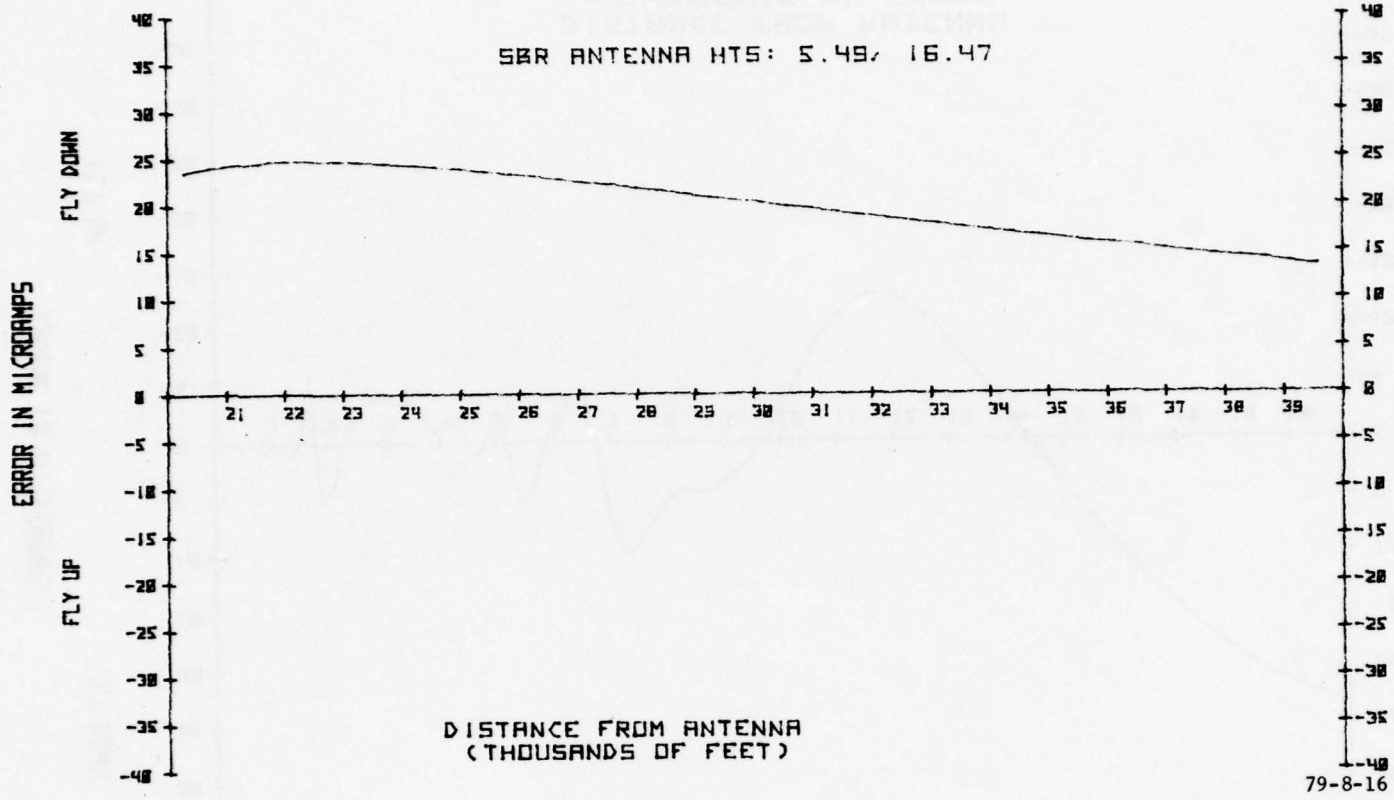


FIGURE 16. SBR ANTENNA, 2.8° GLIDEPATH (40,000 to 20,000 FT)

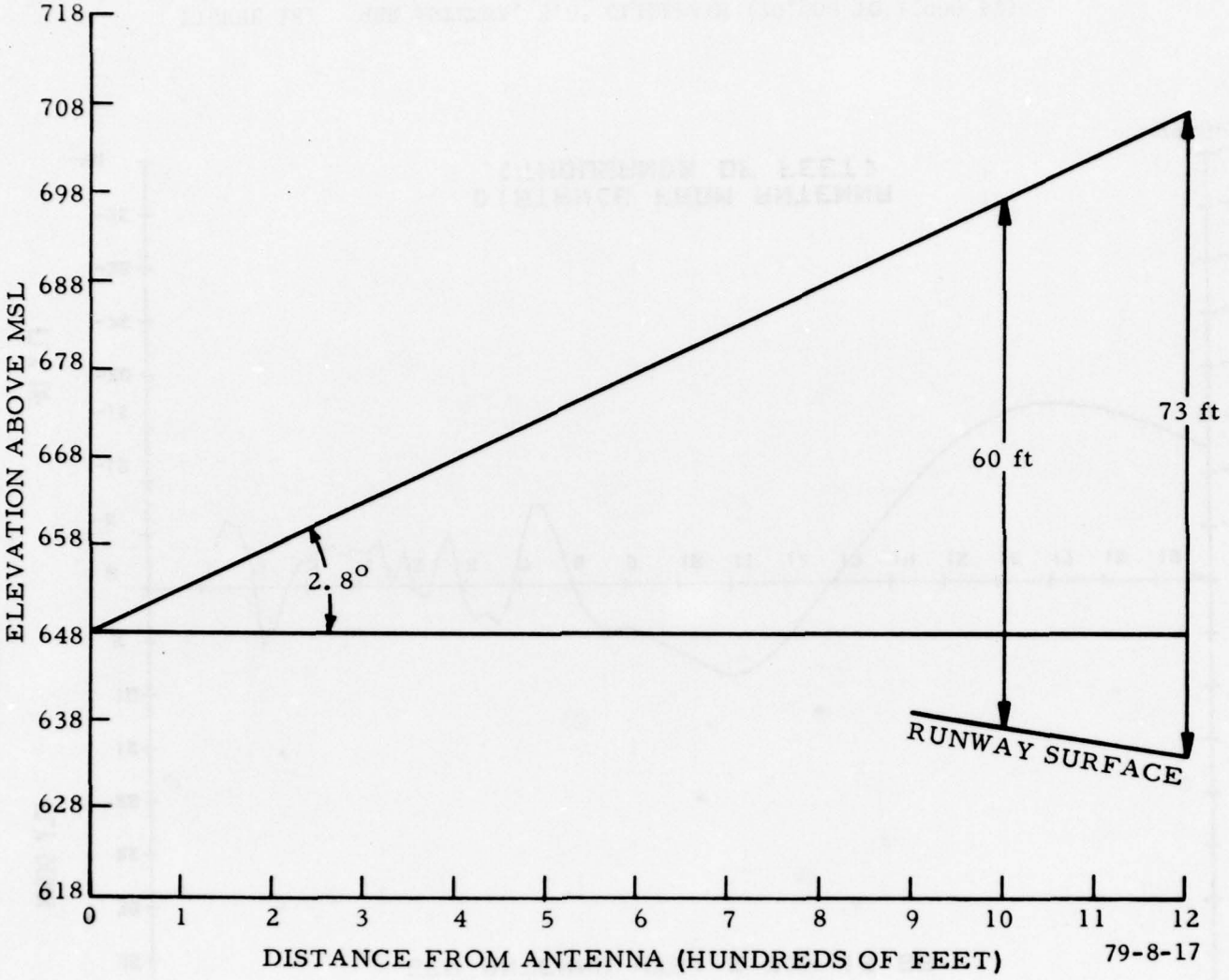


FIGURE 17. THRESHOLD CROSSING HEIGHTS, ANTENNA LOCATION 1, 2.8° GLIDE SLOPE

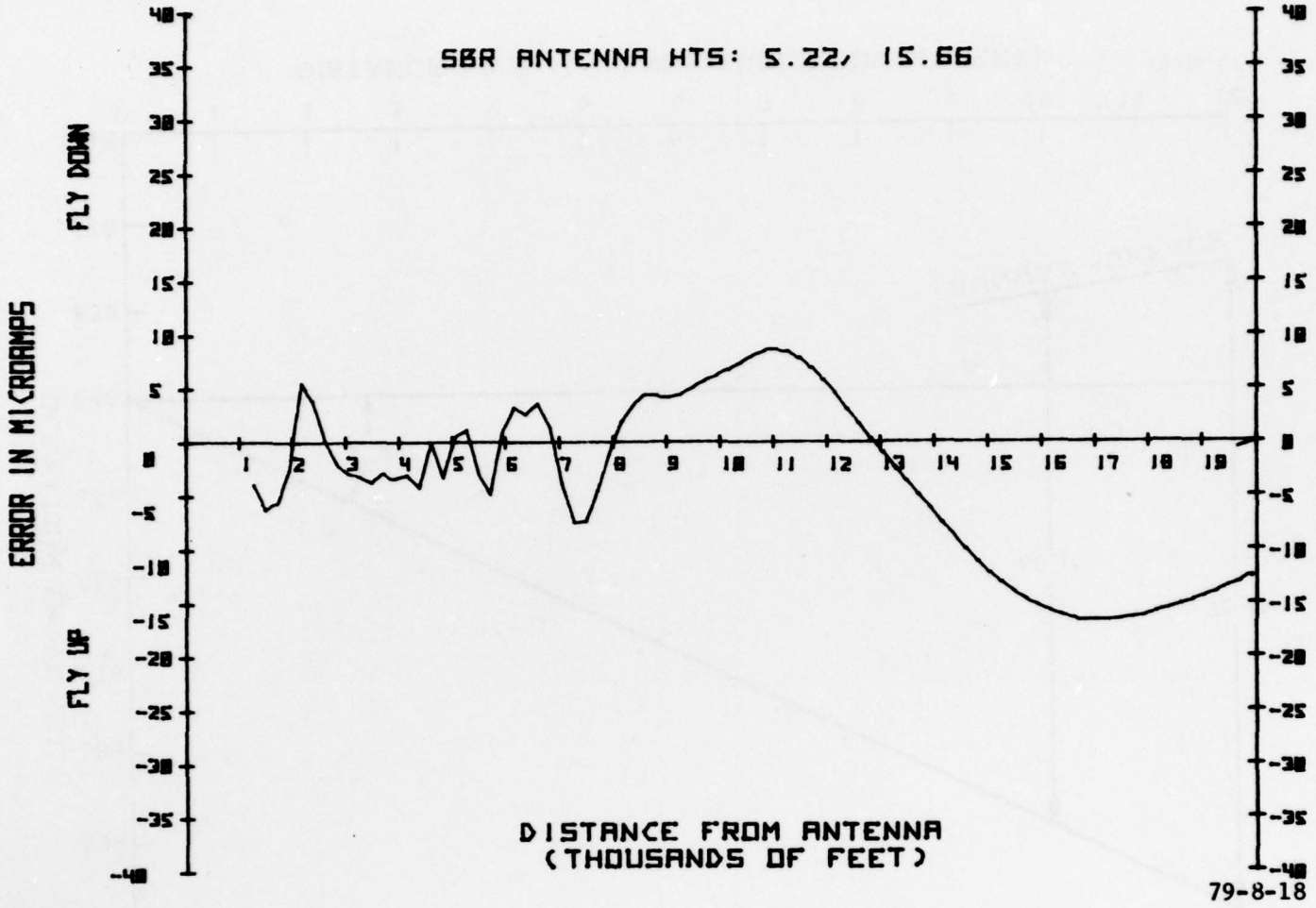


FIGURE 18. SBR ANTENNA, 3.0° GLIDEPATH (20,000 TO 1,000 FT)

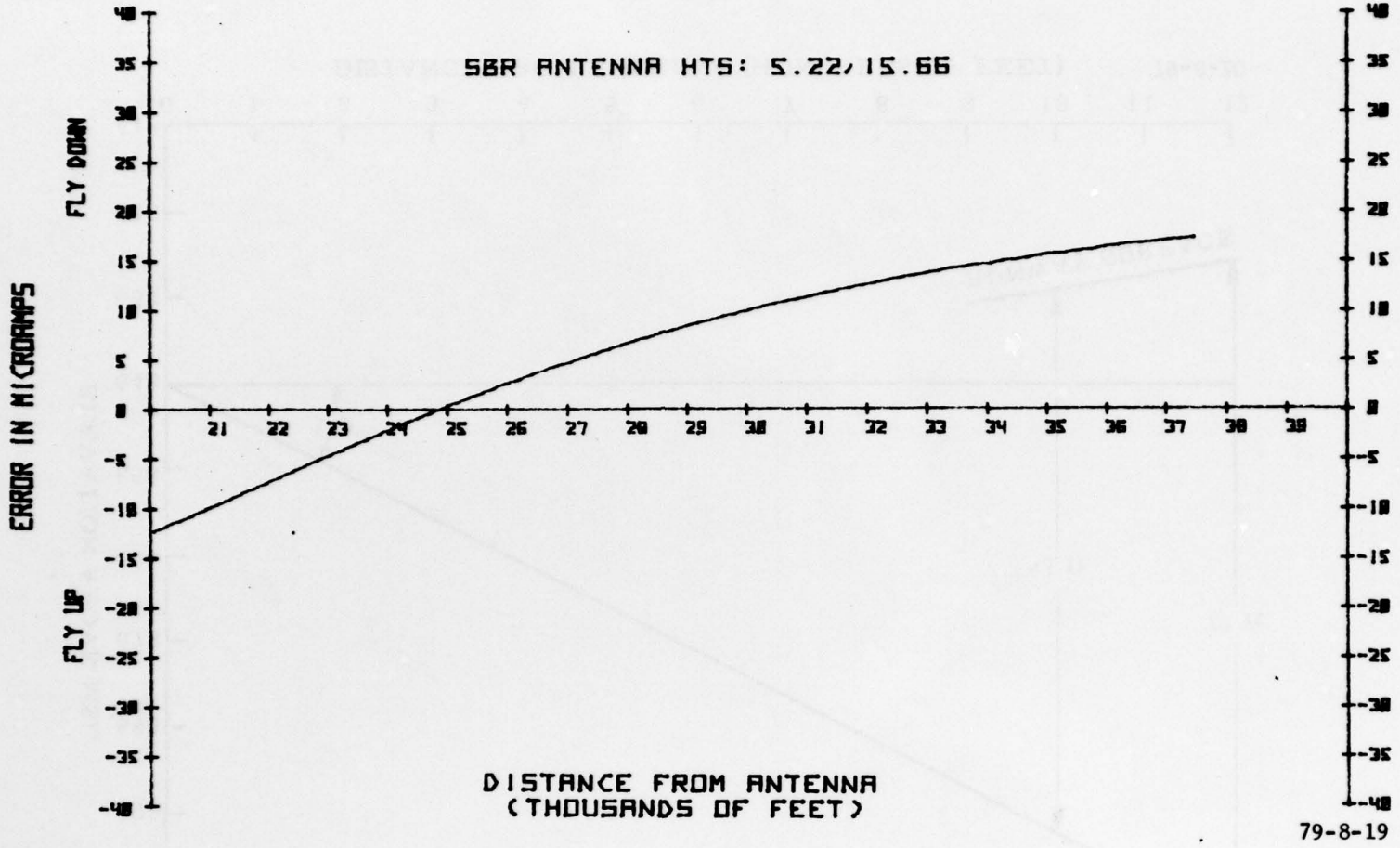


FIGURE 19. SBR ANTENNA, 3.0° GLIDEPATH (40,000 TO 20,000 FT)

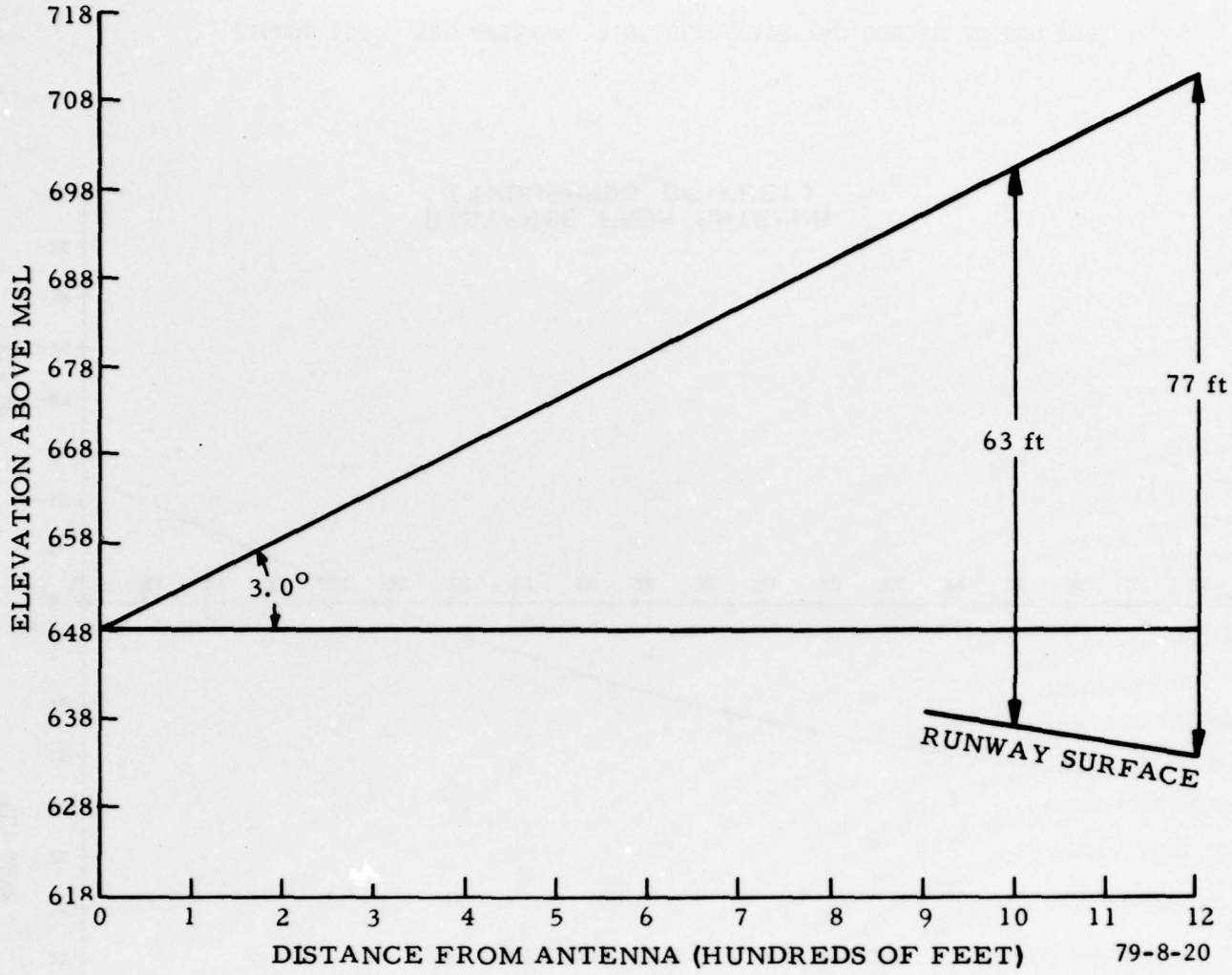


FIGURE 20. THRESHOLD CROSSING HEIGHTS, ANTENNA LOCATION 1, 3.0° GLIDE SLOPE

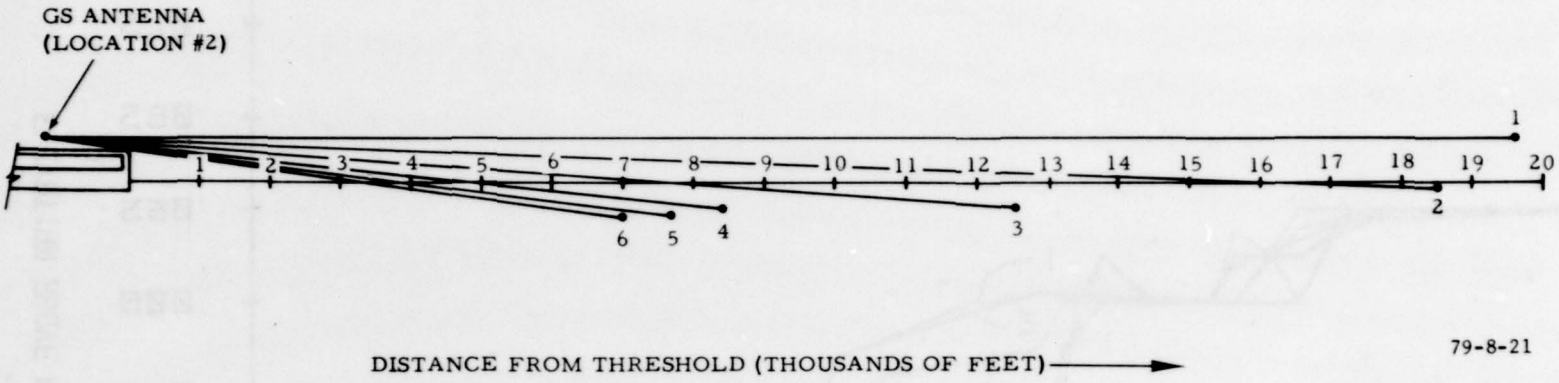


FIGURE 21. PROFILES USED IN MODELING TERRAIN FROM LOCATION NO. 2

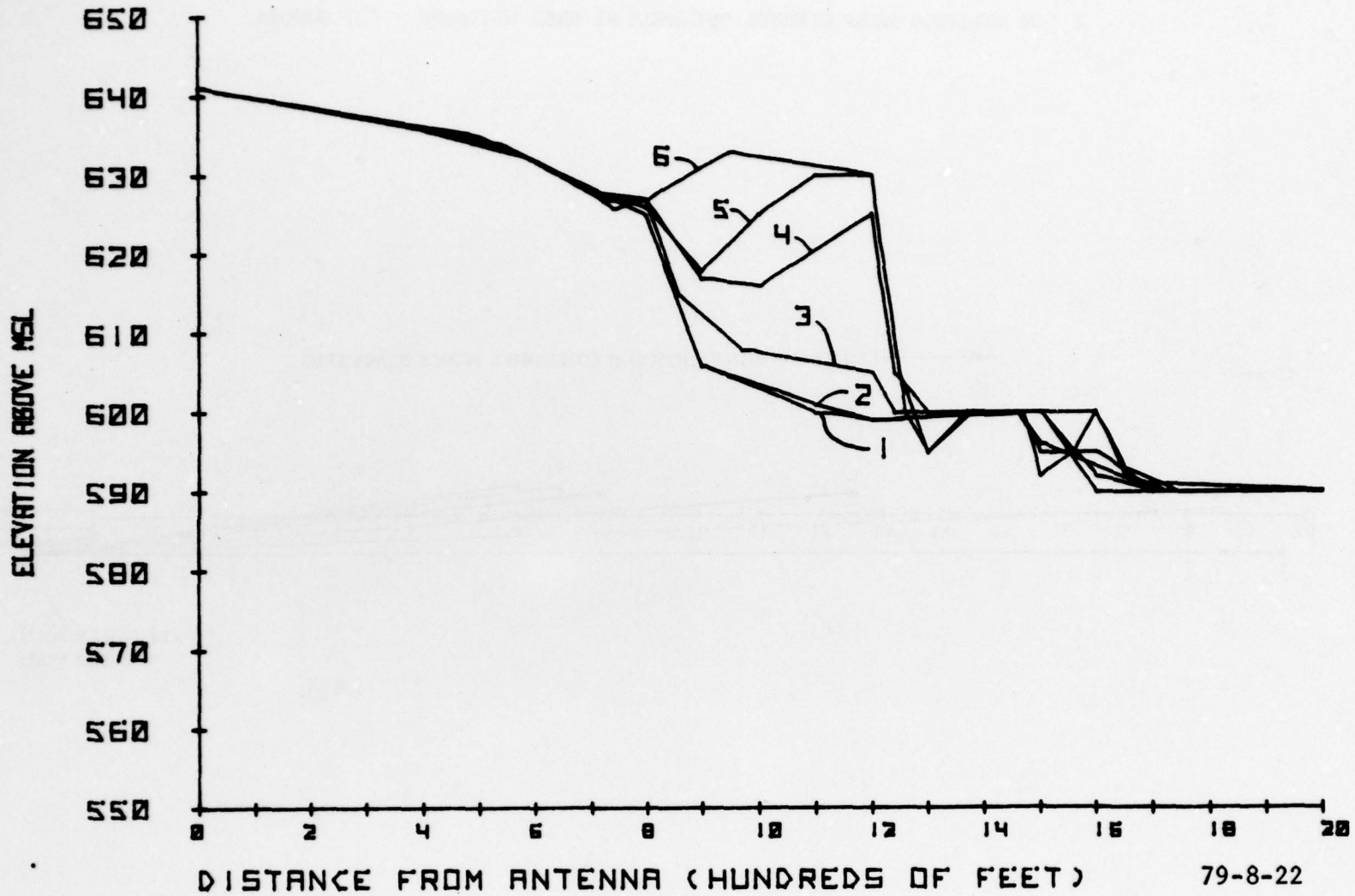


FIGURE 22. TERRAIN PROFILES NOS. 1 THROUGH 6 FOR LOCATION 2

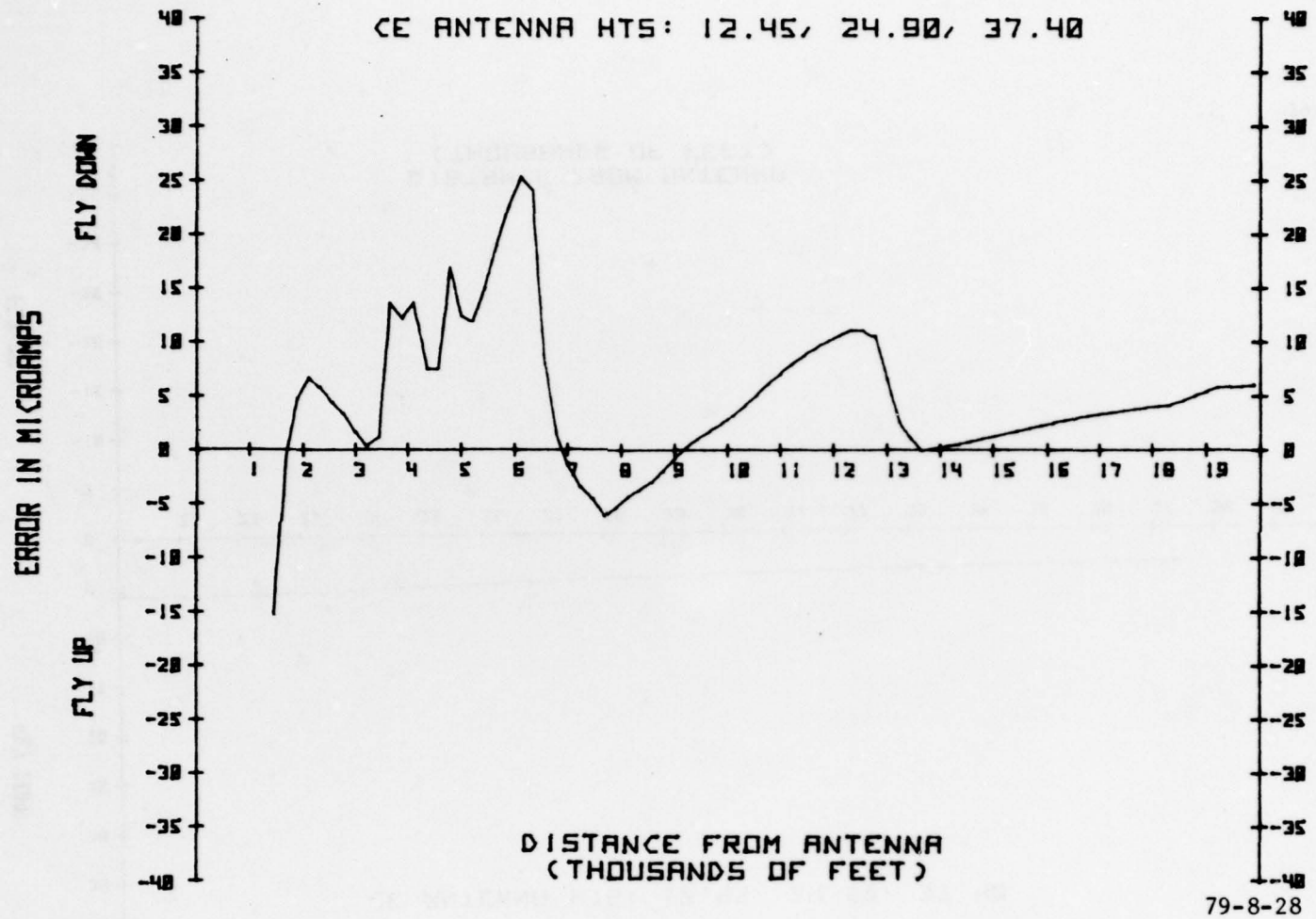


FIGURE 23. CE ANTENNA COMPOSITE PLOT, 2.5° GLIDEPATH (20,000 TO 1,000 FT)

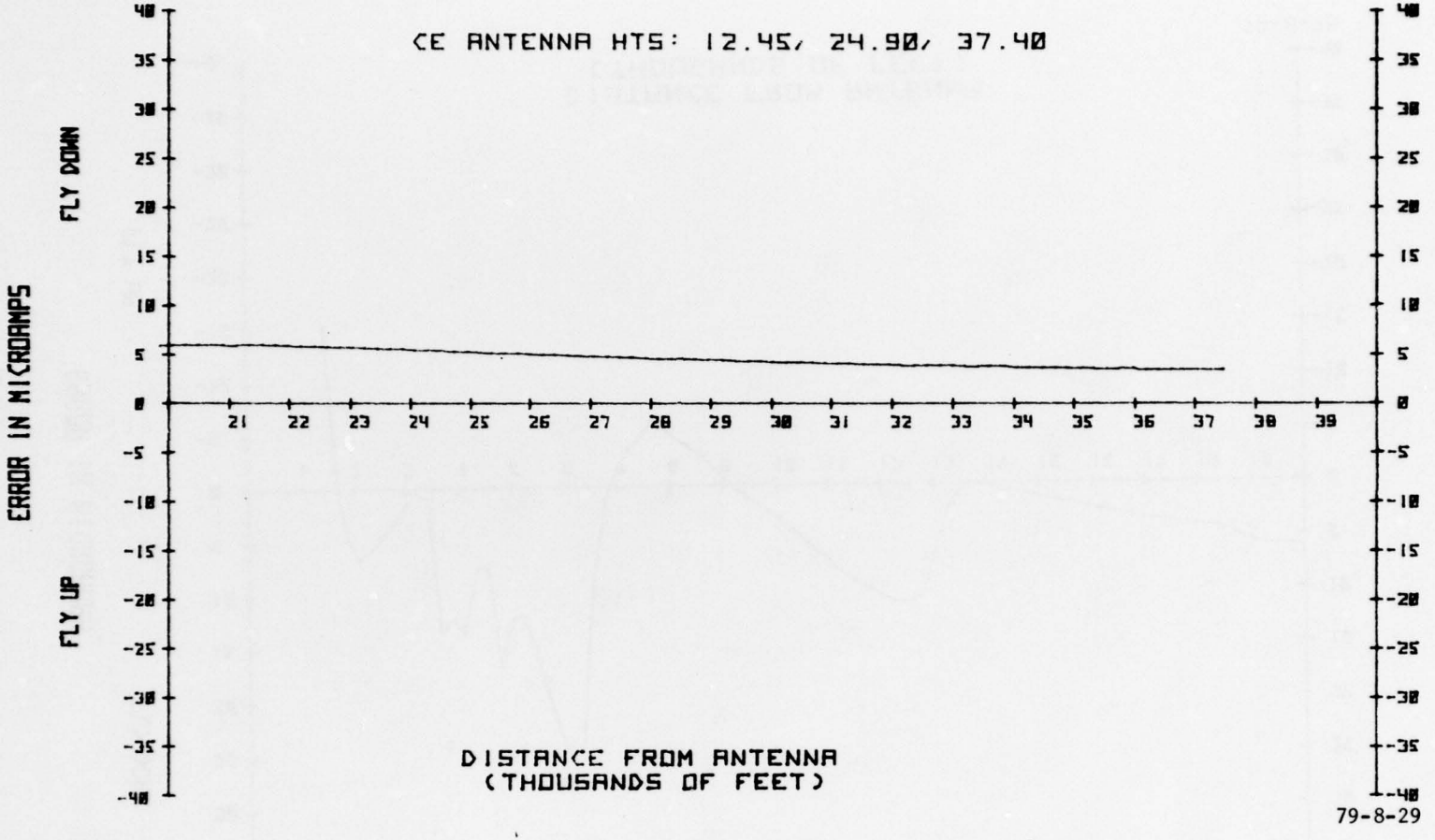


FIGURE 24. CE ANTENNA COMPOSITE PLOT, 2.5° GLIDEPATH (40,000 TO 20,000 FT)

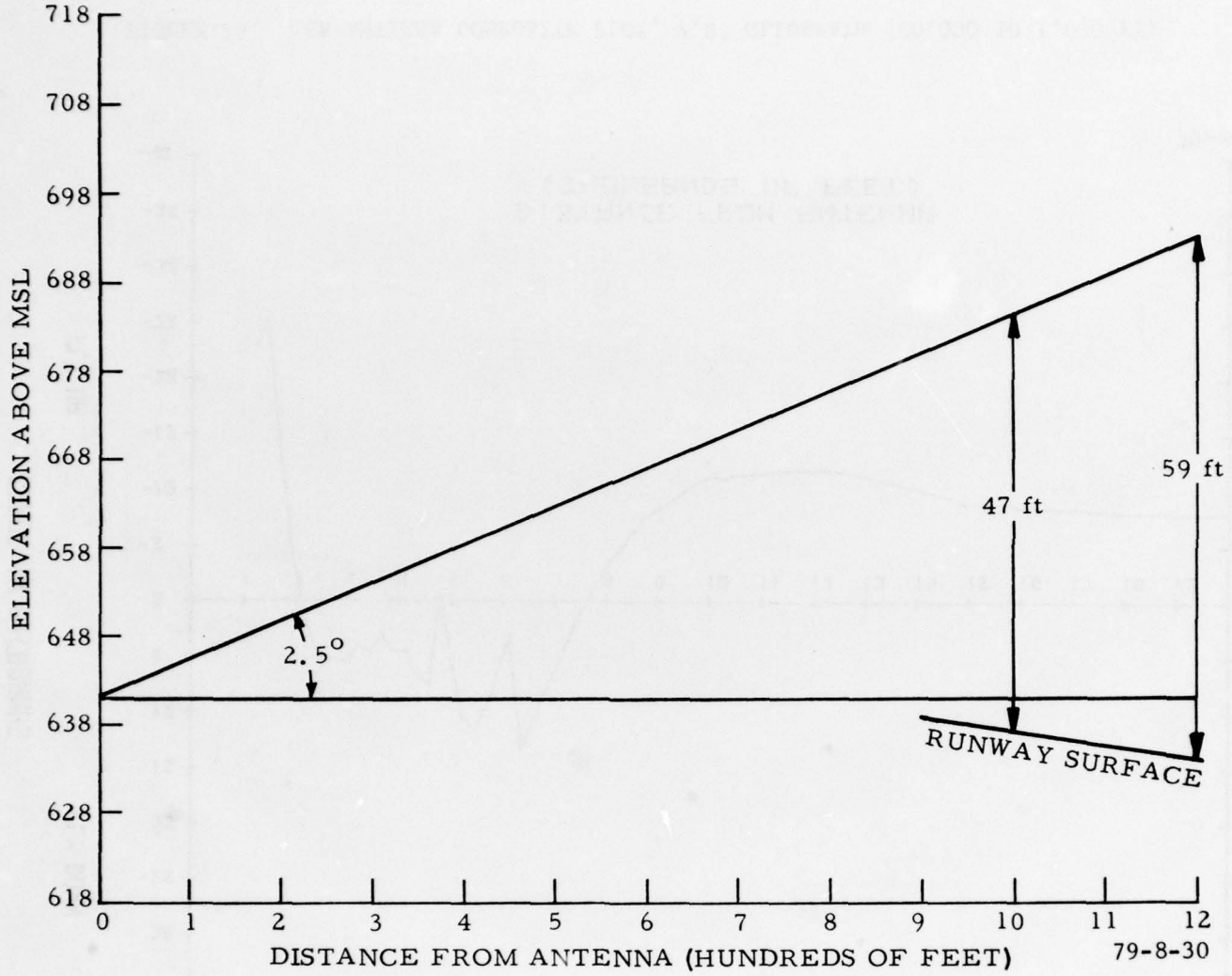


FIGURE 25. THRESHOLD CROSSING HEIGHTS, ANTENNA LOCATION 2, 2.5° GLIDE SLOPE

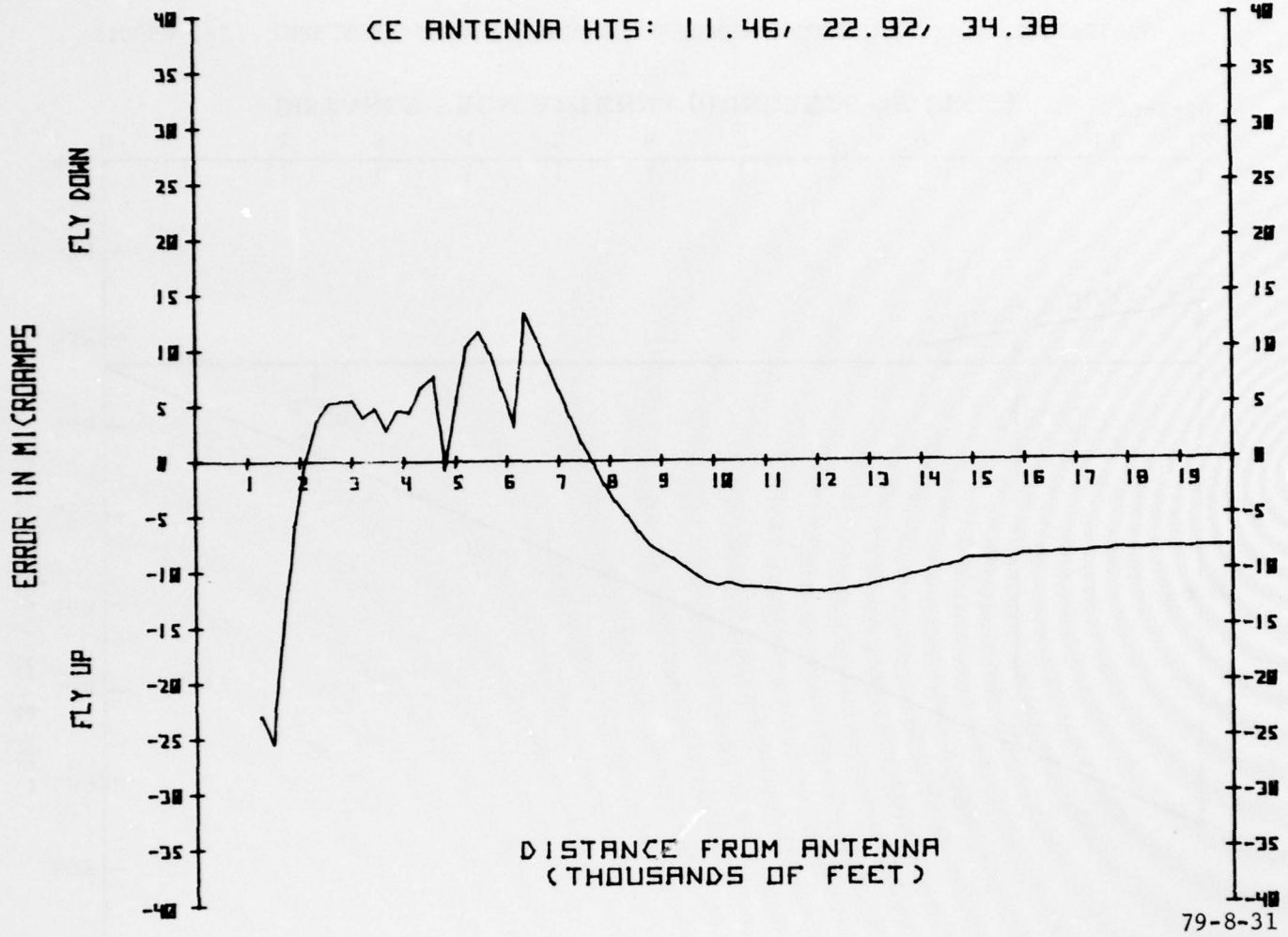


FIGURE 26. CE ANTENNA COMPOSITE PLOT, 2.8° GLIDEPATH (20,000 TO 1,000 FT)

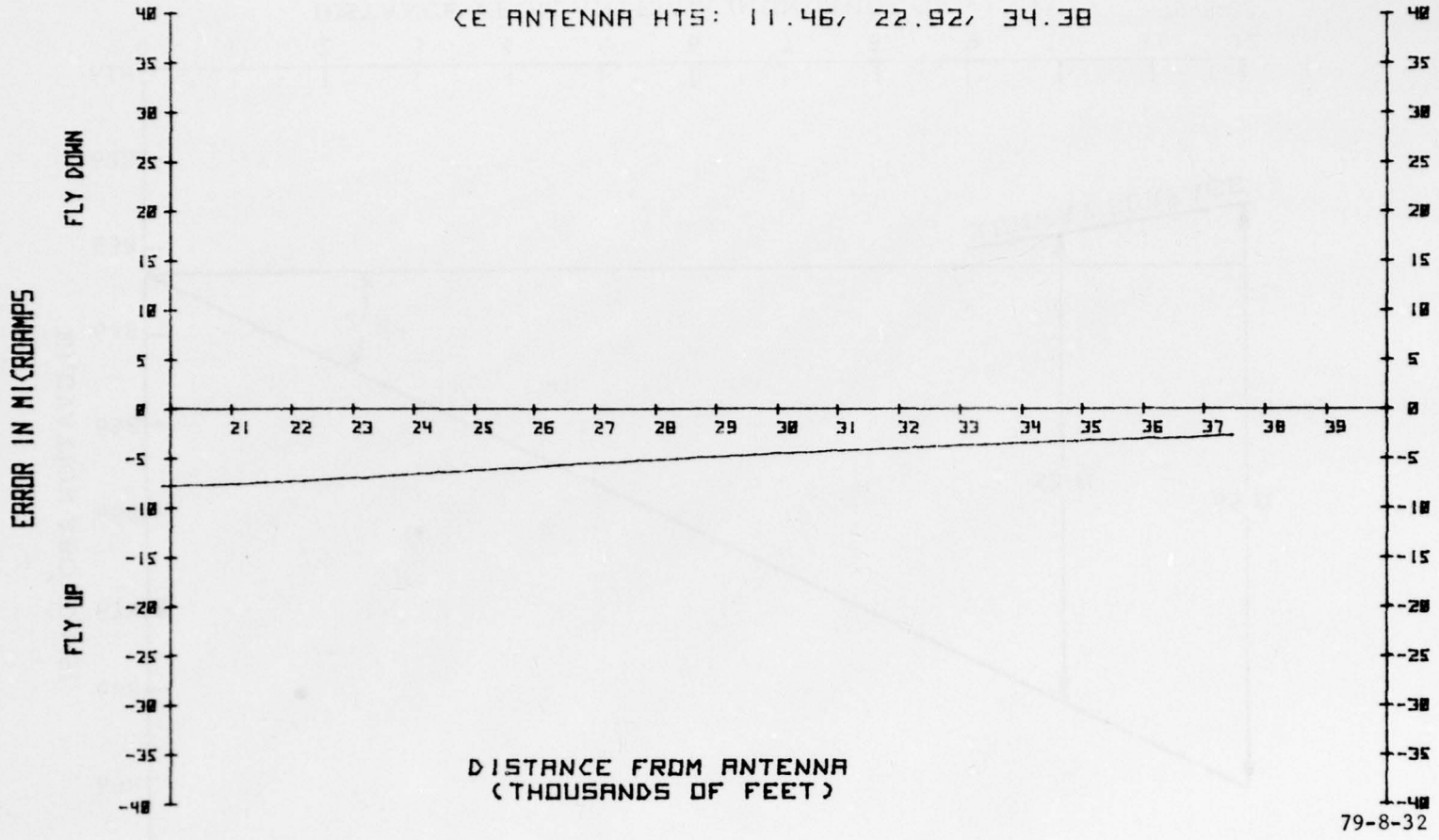


FIGURE 27. CE ANTENNA COMPOSITE PLOT, 2.8° GLIDEPATH (40,000 TO 20,000 FT)

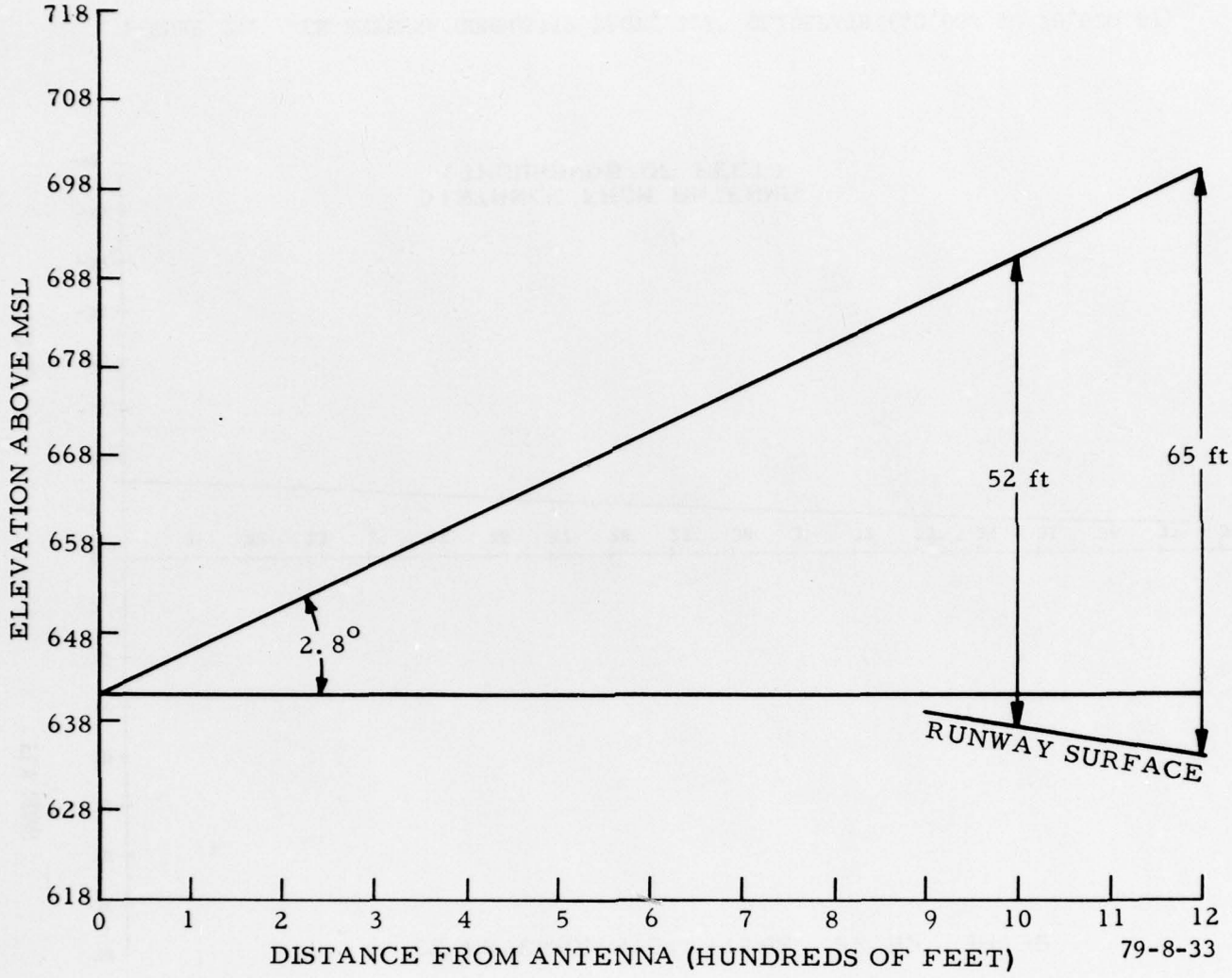


FIGURE 28. THRESHOLD CROSSING HEIGHTS, ANTENNA LOCATION 2, 2.8° GLIDE SLOPE

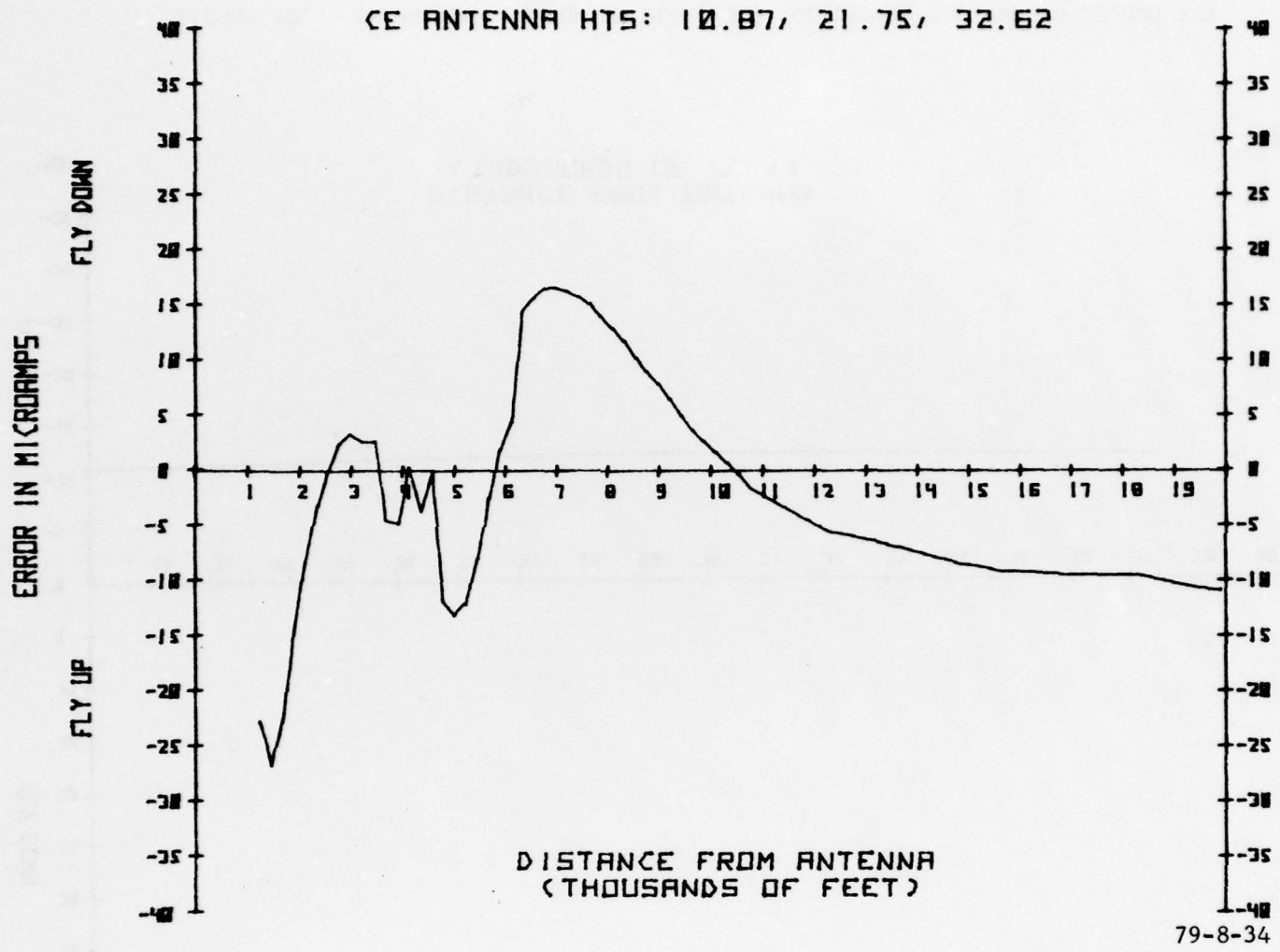


FIGURE 29. CE ANTENNA COMPOSITE PLOT, 3.0° GLIDEPATH (20,000 TO 1,000 FT)

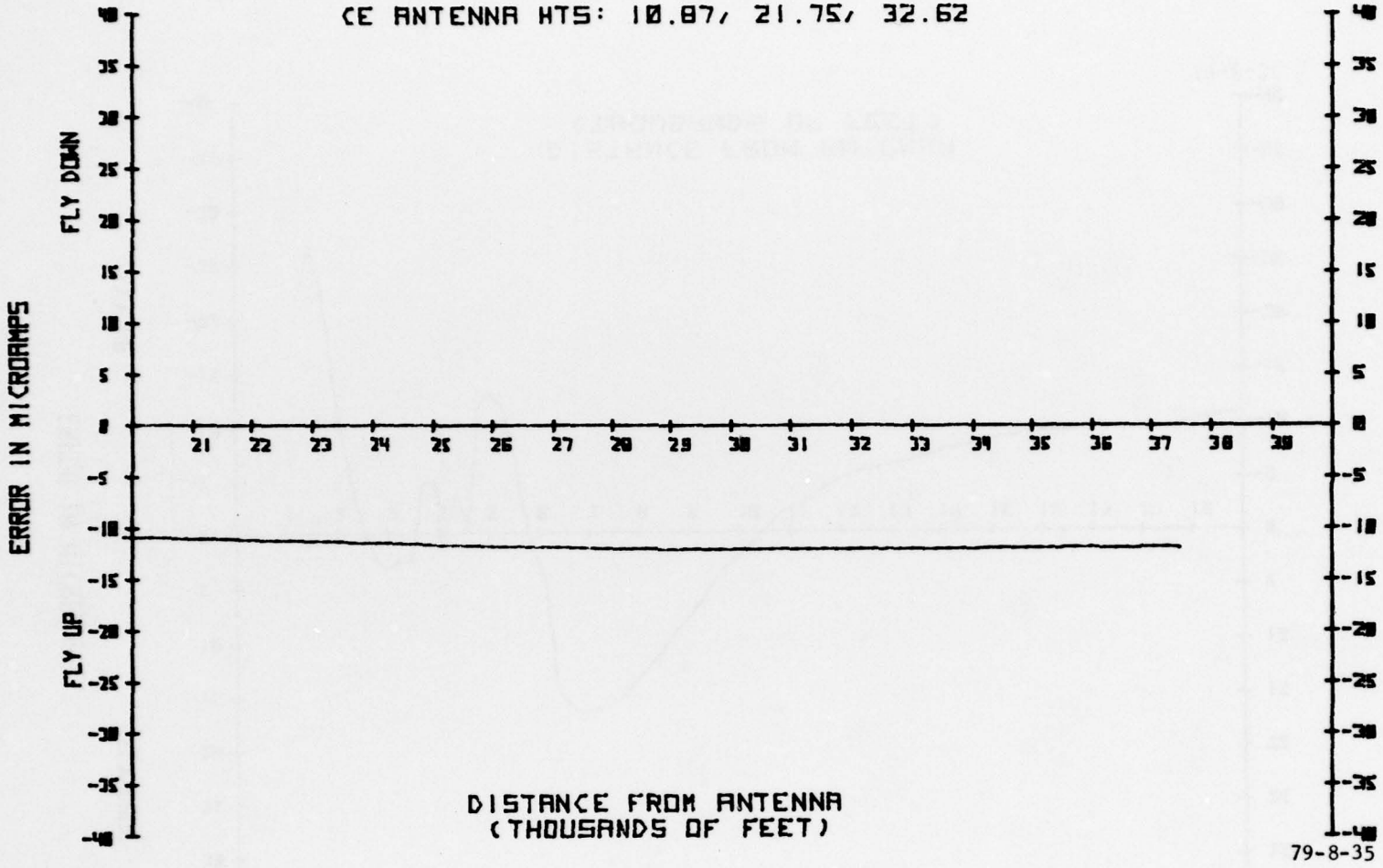


FIGURE 30. CE ANTENNA COMPOSITE PLOT, 3.0° GLIDEPATH (40,000 TO 20,000 FT)

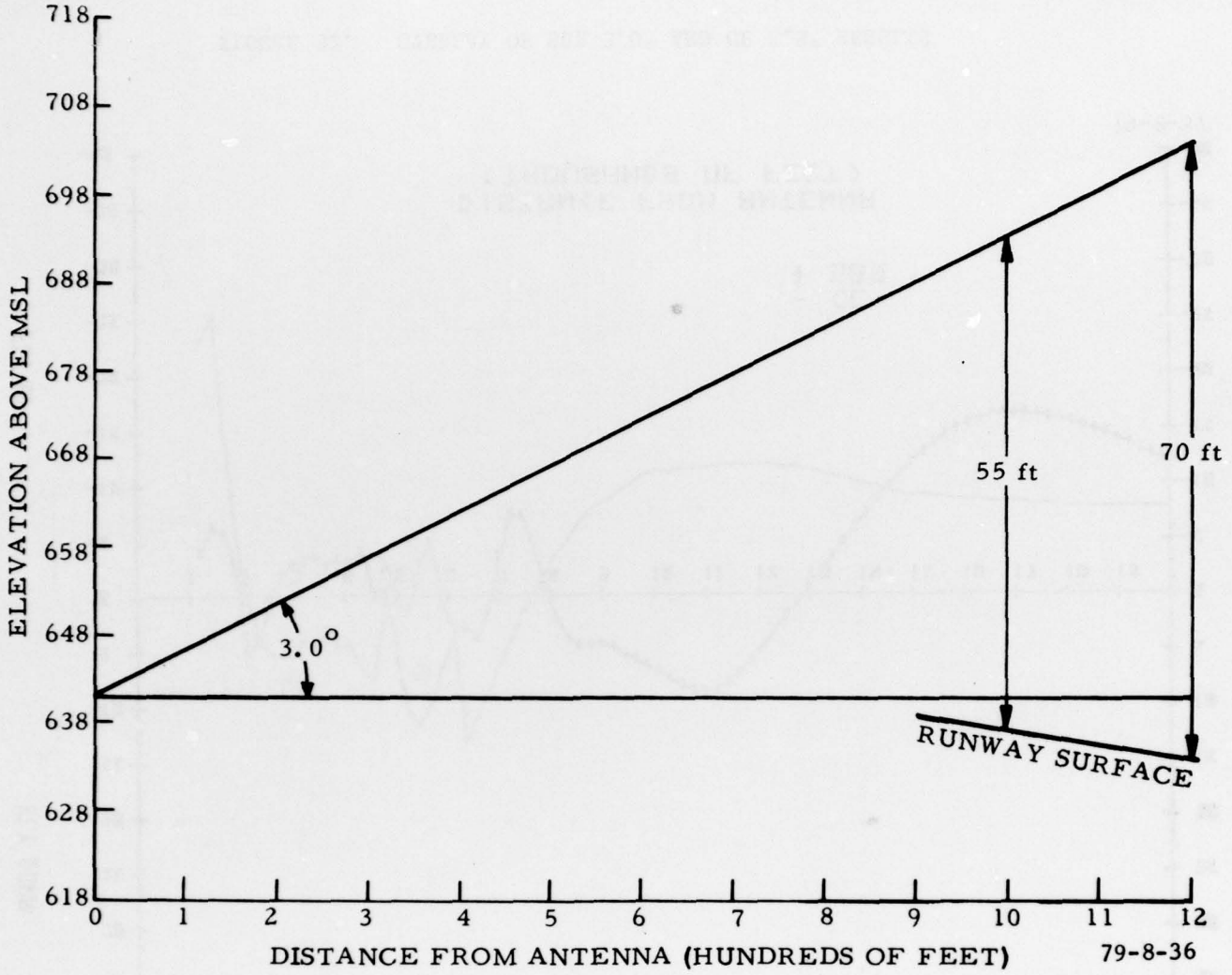


FIGURE 31. THRESHOLD CROSSING HEIGHTS, ANTENNA LOCATION 2, 3.0° GLIDE SLOPE

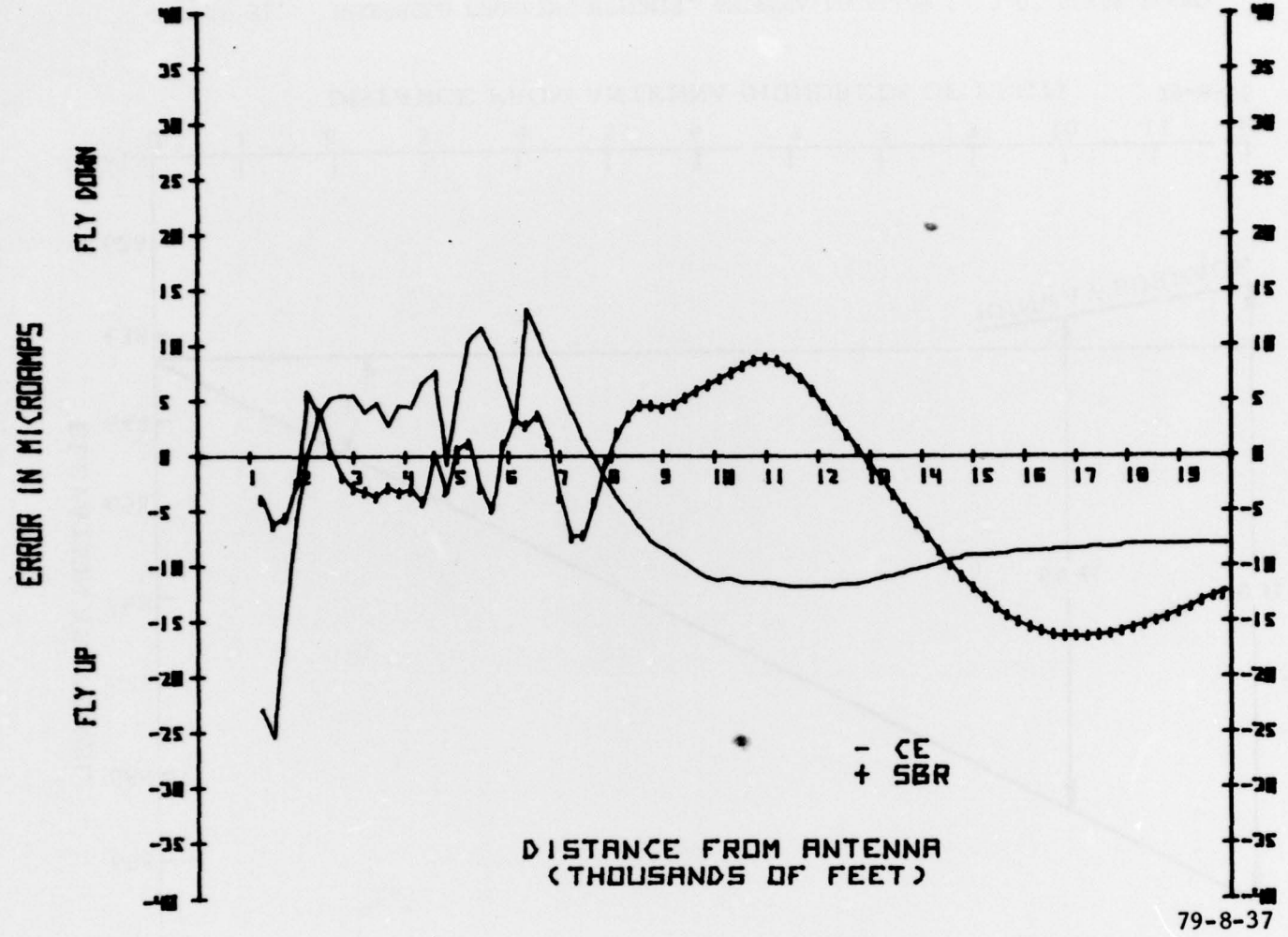


FIGURE 32. OVERLAY OF SBR 3.0° AND CE 2.8° RESULTS